ASCE

Ped-MP: A Pedestrian-Friendly Max-Pressure Signal Control Policy for City Networks

Te Xu, Ph.D.[1]; Yashveer Bika[2]; and Michael W. Levin[3]

Abstract: Decentralized traffic signal controls, such as max-pressure (MP) control, also known as back-pressure (BP) control, have received increased attention recently. MP signal control has been analytically proven to maximize the network throughput and stabilize vehicle queue lengths whenever possible. However, previous work on MP signal control with cyclic and noncyclic phases did not include pedestrian access, which may increase pedestrians' travel time, and delay or even encourage some dangerous behaviors like jaywalking. Because the movement of pedestrians is a nonnegligible factor in traffic management, and many urban planning researchers have found that walking space and walking continuously have significant health, safety, and environmental impacts, a pedestrian-friendly MP signal control policy is needed. Here, we propose a novel pedestrian-friendly MP signal control, Ped-MP, that considers pedestrian access in an urban network to achieve both maximum stability for private vehicles and a comfortable, safe walking experience. This study modifies the original MP control to include pedestrians' access for the first time. Furthermore, this policy still inherits the decentralized property of original MP control, which means it only relies on the local information of individual intersections. Simulation studies are implemented on a popular benchmark network, the Sioux Falls network, with added pedestrians network. The results indicate that, although considering pedestrians' access may reduce the stable region for vehicles, the pedestrians' travel time and delay can be reduced significantly. **DOI: 10.1061/JTEPBS.TEENG-7956.**

Introduction

Intersections controlled by traffic signals are a major bottleneck for traffic in many urban road networks. Consequently, effective timing of traffic signals is highly important for improving traffic flow and reducing vehicle pollutants in cities (Liang et al. 2023; Ma et al. 2021). Decentralized traffic signal controls, such as back-pressure based (BP-based) control, also known as max-pressure (MP) control, have received increased attention recently (Wuthishuwong and Traechtler 2013; Varaiya 2013; Levin et al. 2020; Xu et al. 2022b; Xu 2023). To avoid duplicated definitions and confusion, we use MP control to refer to back-pressure (BP) control and max-pressure (MP) control in the remainder of the paper. One important property of MP control is that it is proven to serve all demand whenever possible. MP control is also decentralized, which means the network-level optimal solution can be found by a local traffic signal controller only using the traffic information from upstream and downstream links (Varaiya 2013; Tassiulas and Ephremides 1990). However, most past MP signal controls with cyclic and noncyclic phases do not include access for multimodal traffic, and thus are not designed for the complex multimodal traffic dynamics in urban areas.

Multimodal traffic is very common in metropolises such as New York City, Chicago, etc., and traffic researchers have therefore focused on multimodal traffic signal timing for decades (He et al. 2012, 2014). Some studies focus on providing better traffic signal timing with pedestrian crossings, given that walking is becoming more and more popular due to the concerns of transportation environmental impacts and increasing travel demand in urban areas (Ma et al. 2015; Zhang et al. 2018; Akyol et al. 2020; Liang et al. 2023). From the perspective of safety, integrating pedestrians' access in signal timing is nonnegligible. DOT (2019) show that there were a total of 6,283 pedestrian fatalities in the United States in 2018, which represents more than a 3% increase from 2017 and the most fatalities since 1990. The risk of pedestrian injuries or fatalities is a significant problem in our transportation systems, which is especially elevated at intersections where vehicle–pedestrian interactions occur (Li et al. 2023a). Therefore, it is important to consider pedestrian access at intersections, especially for the disabled, children, and elderly (Leden et al. 2006; Cafiso et al. 2011; Khosravi et al. 2018). From the point of sustainability and urban planning, promoting walking can result in health benefits (Heinrichs and Jarass 2020; Tang et al. 2021; Park and Garcia 2020). As the critical point to walking accessibility, crosswalks at the intersection provide the connections between sidewalks. Safety and continuous walking space encourage citizens to walk more, which further promotes sustainable development for metropolises. Therefore, we are motivated to find a better signal timing method to provide more friendly signal strategies for pedestrians and serve more vehicles in the urban area.

Many past studies considered public transit and pedestrians in traffic signal optimization problems, and their proposed methods could, to some extent, reduce bus and pedestrian travel time, queue length, and delay. Most of these papers modeled traffic optimization as mixed-integer programming and simulated on a signal intersection or a signal urban corridor, which ignored network-level performance. Furthermore, because most of them belong to centralized signal control (Manolis et al. 2018), these traffic controllers would coordinate adjacent intersections to achieve better

[1]Dept. of Civil, Environmental, and Geo-Engineering, Univ. of Minnesota, Minneapolis, MN 55455; Dept. of Industrial and Systems Engineering, Univ. of Minnesota, Minneapolis, MN 55455 (corresponding author). ORCID: https://orcid.org/0000-0002-9895-6814. Email: te000002@umn.edu

[2]Research Assistant, Dept. of Computer Science and Engineering, Univ. of Minnesota, Minneapolis, MN 55455. Email: bikax003@umn.edu

[3]Assistant Professor, Dept. of Civil, Environmental, and Geo-Engineering, Univ. of Minnesota, Minneapolis, MN 55455. ORCID: https://orcid.org/0000-0002-8778-0964. Email: mlevin@umn.edu

Note. This manuscript was submitted on March 3, 2023; approved on January 16, 2024; published online on April 30, 2024. Discussion period open until September 30, 2024; separate discussions must be submitted for individual papers. This paper is part of the ***Journal of Transportation Engineering, Part A: Systems***, © ASCE, ISSN 2473-2907.

performance but they are hard to implement in urban networks due to high computation time.

MP signal control, often referred to as BP control, stands out as a decentralized signal control method with numerous advantages over traditional approaches. It not only ensures the highest achievable throughput but also operates within a decentralized framework, facilitating independent decision making at each intersection based on localized traffic conditions. Moreover, when serving equal demand levels, MP control typically results in shorter vehicle queues and fewer delays compared to many other control strategies, leading to enhanced vehicular flow, diminished congestion, and improved overall traffic system efficiency. Additionally, MP control is notably adaptive, dynamically adjusting its strategies in response to real-time traffic patterns. While most distributed signal controls, including MP signal control, attempt to address the network implementation challenge predominantly in vehicle-only scenarios, Chen et al. (2020) considered pedestrian access, albeit in the context of autonomous intersection control, not traffic signals. As a result, the integration of MP control with pedestrian access in a predominantly human-driven vehicle environment remains an open research question. Furthermore, integrating pedestrian access into MP control is challenging: First, after integrating pedestrian access, phase timings and turning movement selection will not be purely determined by "pressure" but should measure pedestrian waiting time or waiting queue lengths, which requires significant modification to the signal controller. Second, estimating pedestrian queue lengths at crosswalks near intersections presents challenges due to sensor limitations. While vehicle queues can be accurately gauged using loop detectors, similar sensors specifically designed for pedestrians at intersections are lacking. Modern image-processing technologies are capable of providing reasonably accurate assessments of pedestrian queue lengths. Such advancements may pave the way for a more refined Ped-MP in the future. However, these sensors are not widely used and have significant financial implications, both in terms of initial investment and ongoing maintenance costs, especially when implemented at the network level. Third, behaviors of pedestrians and vehicles are different—i.e., a small number of pedestrians may have unpredictable risks to the intersections, and capacity constraints for pedestrians are often large enough to be inactive. Fourth, most previous studies lack sufficient pedestrian activation data to fully understand pedestrian queue lengths at most intersections, and it is also hard for the MP to get pedestrian queue length data. Therefore, we provide a reasonable way that tracks pedestrian waiting time and the activation of crosswalks around the intersection as input to the MP controller. Consequently, we modify Varaiya's (2013) MP policy to ensure the maximum throughput of vehicles and with bounded waiting times for pedestrians for the first time, which can reasonably balance network-level vehicle stability and pedestrians' access.

There are four main contributions of this work. (1) We modify Varaiya's (2013) MP control policy to include pedestrian access. (2) We design dynamic queueing models for vehicles and pedestrians. (3) We formulate a conflict region constructor, which is inspired by autonomous intersection control, for the proposed MP policy, to model the conflicts between vehicles and pedestrians. Our proposed conflict region logic can be implemented for some irregular networks and intersections. (4) We analytically prove the MP control policy considering pedestrians can also achieve maximum throughput at the network level.

The remainder of this paper is organized as follows. We first summarize the related research about MP control. We then formulate the network model with pedestrian access, vehicle queueing model, pedestrian queue model, stable network definition, and stable region. These contents are prerequisites for proving maximum stability for MP control. We also propose the Ped-MP and stability analysis. We present the simulation results and, finally, we conclude and discuss experimental results.

Literature Review

In this section, we first review related papers focusing on traffic signals that include pedestrian access. Then we review the existing literature on MP signal control and BP signal control.

Traffic Signal Control Including Pedestrian Access

It is worth mentioning that, compared with vehicle traffic, pedestrian traffic is far more complex and random (Ma et al. 2015; He et al. 2012, 2014), especially at intersections. For instance, pedestrians have random routes around intersections and may expose themselves to vehicles. Researchers have been focusing on pedestrians' movements for a long time, with some of them focusing on providing convenient infrastructure for children, the elderly, and the disabled, who have lower walking speeds (Leden et al. 2006; Cafiso et al. 2011; Khosravi et al. 2018). Some researchers wanted to provide better walking spaces in the cities from the perspective of urban planners (Hooper et al. 2018). A walkable city (city with enough walking spaces) has many benefits, such as social, environmental, and economic benefits. Specifically, a city that has better walking space can encourage residents to embrace walking rather than driving a vehicle, which fosters community connections and reduces greenhouse gas emissions. Recently, many urban planners who focus on public spaces proposed that we should balance street space for pedestrians and vehicles. They proposed three ways to balance street space: (1) improving pedestrian flow, (2) providing space for pedestrian amenities, and (3) making it easier to cross the street. The first and third points are determined by the traffic signal controller. Akyol et al. (2020) proposed an adaption of the original split, cycle, and offset optimization technique (SCOOT) to accommodate vehicle and pedestrians traffic. Using simulations in PTV-VISSIM, they found that a tradeoff exists between pedestrian travel time and vehicle delay. Ma et al. (2015) established quantitative standards, which consider safety and efficiency tradeoff factors for selecting pedestrian phases for signalized intersections, and results showed that their technology can select pedestrian phases properly. Zhang et al. (2018) provided a traffic light scheduling model for a pedestrian–vehicle mixed-flow traffic environment. The proposed model is a mixed-integer linear program that can achieve a good balance between pedestrian demand and vehicle demand. Zhang et al. (2019) also formulated a more realistic model, the pedestrian-safety-aware traffic light strategy, in which pedestrian arrival flow and leaving flow are separately described. Based on a genetic algorithm (GA) and the harmony search, their model performed better than traditional adaptive signal control methods.

Some researchers started to pay more attention to future traffic environments with pedestrian access. Xu et al. (2022a) pointed out that, although vision technologies can be applied to intersection control that integrates pedestrian access, the movement of pedestrians is hard to determine. To solve this problem, they suggested that 6G localization and tracking services offer traffic engineers new opportunities, and proposed a traffic signal control policy for pedestrians and vehicles under 6G future technology. He et al. (2012) leveraged the advantage of online data to identify the vehicle platoon and combine the request from special vehicles (public transit) to formulate a mathematical programming problem to predict future signal states. Although they did mention pedestrian access, they modeled requests for special vehicles by replacing with pedestrian crossing requests. Later on, He et al. (2014) proposed a

multimodel traffic signal control policy including signal actuation and coordination, which includes pedestrian access. They built simulations on a corridor and found that their method can reduce pedestrian delay and average passenger delay. However, most of these studies tried to model traffic signal optimization problems as mixed-integer programs, which are computationally difficult to implement at the network level.

MP Signal Control

MP signal control, also known as BP signal control, is one type of decentralized signal control method. MP was proposed for scheduling in communication and power systems (Tassiulas and Ephremides 1990). Varaiya (2013) converted it into a traffic signal control and proved that the proposed MP signal controller can ensure that the transportation network is stable whenever possible. They modeled the traffic state based on the vehicle queue lengths. Many other papers extended the research of Varaiya (2013). Gregoire et al. (2014a) proposed a BP traffic signal control and proved it can achieve stability based on Lyapunov drift with corresponding simulation results. Later, Gregoire et al. (2014b) developed another BP traffic signal control that considers road capacity, which can better handle congestion in the network.

Due to the complexity of the proof of maximum stability, many past studies did not characterize the stable demand region and provide a rigorous proof of stability (Sun and Yin 2018; Chang et al. 2020; Yu et al. 2021). For example, Sun and Yin (2018) compared the noncyclic MP (Varaiya 2013) signal controller, cyclic MP signal controller, and coordinated actuated traffic signal controller with simulation in VISSIM based on realistic scenarios. Their results showed that the cyclic-based MP signal control had worse performance than noncyclic MP signal control, and noncyclic MP signal control achieves better performance than the coordinated actuated traffic signal controller currently in use. Some researchers tried to modify the original MP traffic control, which models traffic dynamics as vehicles' queue length. For instance, Mercader et al. (2020) proposed a novel travel-time based MP traffic control. Dixit et al. (2020) proposed an MP signal control with signal timing based on crowd-sourced delay data. Although these works gave us inspiration for implementation and modification of MP signal controls, they lacked a proof of the maximum stability property.

To encourage the practical implementation of MP signal control, many studies provided modified structures for MP signal control. Le et al. (2015) and Levin et al. (2020) proposed cyclic-based MP signal controls, as the original MP signal control (Varaiya 2013) activates phases in arbitrary order and may cause a long waiting time for vehicles in the low-demand direction, and provided rigorous proofs of stability. To test the performance of cyclic-based MP signal control, Barman and Levin (2022) provided a performance evaluation with modified cyclic-based MP signal control in two realistic corridors, showing that the modified cyclic-based MP signal control can reduce vehicle delay compared with current signal control in Minneapolis, Minnesota. Some researchers wanted to leverage emergency connected and autonomous vehicle technologies (Tu et al. 2019; Xu et al. 2021; Ma and Wang 2021; Ma et al. 2022; Xu et al. 2023). For instance, Liu and Gayah (2022) proposed a novel delay-based MP controller, where their delay is defined as the total vehicles' stopped time in a road link. Their proposed MP signal control method can achieve better delay performance when connected and autonomous vehicles are more widely available. Rey and Levin (2019) also introduced the concept of the blue phase to switch between traffic signals and autonomous intersection management while retaining maximum throughput. In addition, the original MP signal control (Varaiya 2013) is based on the point-queue model (Vickrey 1969; Zhang et al. 2013), which is unrealistic. Therefore, some researchers started developing MP signal controllers that can capture the spatial distribution of traffic dynamics over road links for more accurate MP signal timing. For example, Li and Jabari (2019) proposed a position-weighted BP signal control policy based on a more accurate model of traffic flow. However, their proposed method is hard to implement in reality, because we cannot obtain accurate density information over every continuous space of a link. Xu et al. (2022c) proposed an approximated method to obtain density information. With the emergence of artificial intelligence, many researchers tried to leverage reinforcement learning (RL) knowledge to MP control (Wei et al. 2019; Yang et al. 2019; Maipradit et al. 2021; Yang et al. 2019; Ke et al. 2020; Wang et al. 2022; Zheng et al. 2023). Chen et al. (2020) was the first paper that incorporated pedestrians and MP-based signal control, but their proposed method was only suitable for the environment of fully autonomous vehicles (non-signal structure) and the simulation was implemented on a grid-based network without considering realistic pedestrian phase design. Considering the aforementioned research and the demand for pedestrians' intersection access, we extend the MP policy to consider the access of pedestrians in a realistic network.

Problem Formulation

Road Network Model with Pedestrian Access

Consider an urban network $\mathcal{G} = (\mathcal{N}, \mathcal{A})$ with nodes $\mathcal{N}$ and links $\mathcal{A}$. We separate the urban network into the vehicle network $\mathcal{G}^{\mathrm{v}} = (\mathcal{N}^{\mathrm{v}}, \mathcal{A}^{\mathrm{v}})$ and the pedestrian network $\mathcal{G}^{\mathrm{p}} = (\mathcal{N}^{\mathrm{p}}, \mathcal{A}^{\mathrm{p}})$, because vehicles move along the road and pedestrians move through the sidewalks and crosswalks, and they will interact with each other at intersections. Nodes represent intersection locations. Nodes $\mathcal{N}$ are divided into vehicle nodes (intersections) $\mathcal{N}^{\mathrm{v}}$ and pedestrian nodes (intersections) $\mathcal{N}^{\mathrm{p}}$. The link set $\mathcal{A}$ is divided into three subsets, which are the entry link set $\mathcal{A}_e$, the internal link set $\mathcal{A}_i$, and the exit link set $\mathcal{A}_o$. Specifically, entry link set $\mathcal{A}_e$ can be divided into pedestrian entry links $\mathcal{A}_e^{\mathrm{p}}$ and vehicle entry links $\mathcal{A}_e^{\mathrm{v}}$; internal link set $\mathcal{A}_i$ are composed of vehicle internal links and $\mathcal{A}_i^{v}$ and pedestrian internal links $\mathcal{A}_i^{\mathrm{p}}$; and exit link set $\mathcal{A}_e$ are composed of vehicle exit links and $\mathcal{A}_e^{\mathrm{v}}$ and pedestrian exit links $\mathcal{A}_e^{\mathrm{p}}$. Note that entry links and exit links are not realistic links, which are used for loading and removing vehicles and pedestrians. Entry links are the those where pedestrians and vehicles can enter the network, which are modeled as point queues. Exit links are the sink links where pedestrians and vehicles leave the network once they reach their destination nodes.

For the vehicle network $\mathcal{G}^{\mathrm{v}} = (\mathcal{N}^{\mathrm{v}}, \mathcal{A}^{\mathrm{v}})$, internal links $\mathcal{A}_i^{\mathrm{v}}$ connect the intersections located inside the vehicle network. We define $\mathcal{M}$ be the set of all turning movements in the network. We use Γ_i^+ and Γ_j^+ to represent the sets of outgoing links and incoming links of nodes (intersections), respectively. One turning movement is a combination of two links. For instance, (i, j) and (j, k) are two movements, respectively. Let $x_{ij}^{\mathrm{v}}(t)$ be the number of vehicles on link i waiting to move to link j. Let $d_i^{\mathrm{v}}(t)$ be the vehicles' demand entering the network on link $i \in \mathcal{A}_e$ at time t, which are an independent identically distributed random variable with average value $\overline{d}_i^{\mathrm{v}}$. Turning proportion $r_{jk}^{\mathrm{v}}(t)$ is the proportion of vehicles entering link j that will next move to link k at time t, which are independent identically distributed random variables with mean $\overline{r}_{ij}^{\mathrm{v}}$. Usually, the turning proportions can be obtained from historical travel data. We separate the vehicle queues on the link by turning movements, as in previous work (Varaiya 2013).

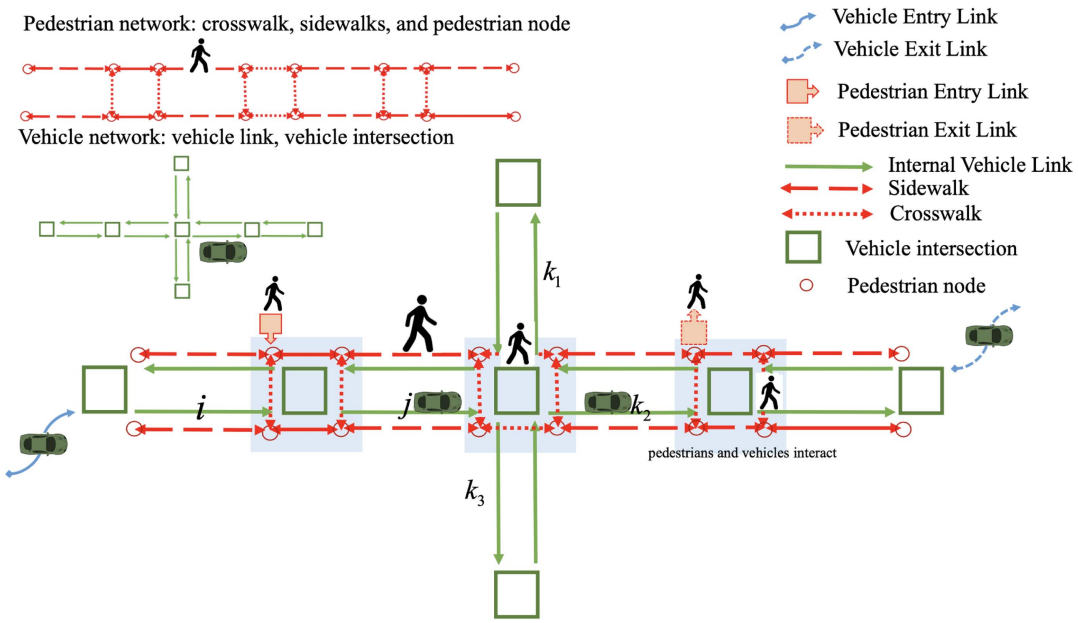

Fig. 1. Network with pedestrian access.

For the pedestrians network $\mathcal{G}^{\mathrm{p}} = (\mathcal{N}^{\mathrm{p}}, \mathcal{A}^{\mathrm{p}})$, the pedestrian links represent the sidewalks and crosswalks. Note that pedestrian nodes (intersections) $\mathcal{N}^{p}$ are not the physical intersections, but rather the nodes to connect sidewalks and crosswalks. Let $x_{ij}^{\mathrm{p}}(t)$ be the number of pedestrians on link i waiting to move to link j. Let $d_i^{\mathrm{p}}(t)$ be the pedestrian demand entering the network on link $i \in \mathcal{A}_e$, which are independent identically distributed random variables with average value $\overline{d}_i^{\mathrm{p}}$. Turning proportion $r_{ij}^{\mathrm{p}}(t)$ determines the proportion of pedestrians entering link i that will next move to link j, which are also independent identically distributed random variables with mean $\overline{r}_{ij}^{\mathrm{p}}$. Turning proportion $r_{ij}^{\mathrm{p}}(t)$ determines the proportion of pedestrians entering i that will next move to j, which are independent identically distributed random variables with mean $\overline{r}_{ij}^{\mathrm{p}}$. To focus on the impacts of signal control for pedestrians, we set the speed for pedestrians as constant and the capacity as infinite, which is similar to the point queue model for pedestrian propagation.

To model the vehicle and pedestrian conflicts, we use α_{ij}^{b} to indicate whether the vehicle turning movements (i, j) conflict with pedestrians' movement when pedestrians want to move across the crosswalk b. For vehicles moving through the intersections, the capacity of the conflict region is Q_c, which is determined by the capacities of turning movements, $Q_c = \max_{(i,j)|c\in C_{ij}}\{Q_{ij}\}$. The total number of vehicles driving through one conflict region per time is bounded by the capacity of the conflict region. Additional details can be found in Fig. 1.

Vehicle Queueing Model

To calculate the vehicle queueing propagation in the network under discretized time, we use the store-and-forward model of Varaiya (2013). The evolution of vehicle queueing along an internal link can be mathematically expressed through Eq. (1), which is elucidated in Fig. 2. As depicted in the figure, two vehicles transition from link k_2 and k_3 (upstream) to the downstream link i. Meanwhile, one vehicle moves from link i to link j. Thus, at time t, the queueing state is denoted by $x_{ij}(t) = 3$. Factoring in these movements, the queueing state at the subsequent time instance, $x_{ij}(t+1)$, is computed as $3 - 1 + 2 = 4$

$$x_{ij}^{\mathrm{v}}(t+1) = x_{ij}^{\mathrm{v}}(t) - y_{ij}^{\mathrm{v}}(t) + \sum_{(i,j,h)\in(\mathcal{A}^{\mathrm{v}})^3} y_{hi}^{\mathrm{v}}(t) \times r_{ij}^{\mathrm{v}}(t) \quad (1)$$

where $y_{ij}^{\mathrm{v}}(t)$ = signal controlled flow that starts from link i and then travels to link j. Vehicle flow conservation also applies to entry links with the following equation:

$$x_{ij}^{\mathrm{v}}(t+1) = x_{ij}^{\mathrm{v}}(t) - y_{ij}^{\mathrm{v}}(t) + d_i^{\mathrm{v}}(t) \times r_{ij}^{\mathrm{v}}(t) \quad (2)$$

The activation of vehicle turning movement (i, j) is denoted by $s_{ij}(t) \in \{0, 1\}$. The value of $y_{ij}^{\mathrm{v}}(t)$ is determined by the following equation:

$$y_{ij}^{\mathrm{v}}(t) = \min\{Q_{ij}^{\mathrm{v}} s_{ij}(t), x_{ij}^{\mathrm{v}}(t)\} \quad (3)$$

where Q_{ij}^{v} = capacity of turning movement from link i to link j. Specifically, $Q_{ij}^{\mathrm{v}} = \min(Q_i^{\mathrm{v}}, Q_j^{\mathrm{v}})$ is the maximum flow of vehicle

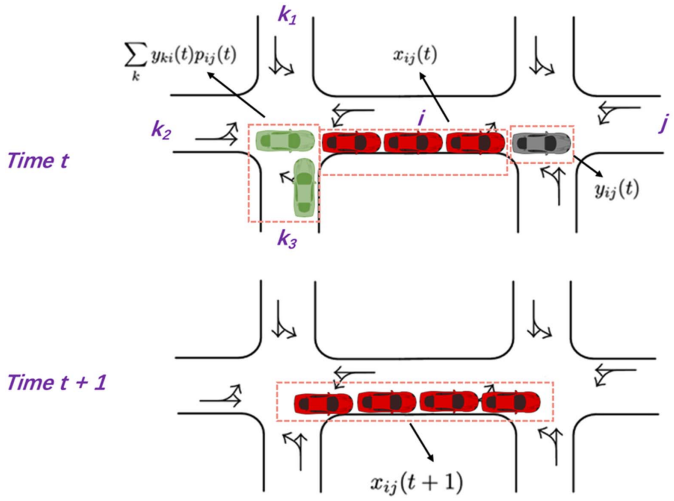

Fig. 2. Vehicle queueing model explanation.

movement (i, j). Note that capacity is the maximum road throughput, which we assume to be constant for each link.

Pedestrian Queueing Model

To track the propagation of pedestrians queueing in the network, we construct a store-and-forward queueing model, which is also inspired by Varaiya (2013)

$$x_{ij}^{\mathrm{p}}(t+1) = x_{ij}^{\mathrm{p}}(t) - y_{ij}^{\mathrm{p}}(t) + \sum_{(i,j,h)\in(\mathcal{A}^{\mathrm{p}})^3} y_{hi}^{\mathrm{p}}(t) \times r_{ij}^{\mathrm{p}}(t) \quad (4)$$

where $y_{ij}^{\mathrm{P}}(t)$ = flow of pedestrians from i to j at time t, which is controlled by intersection signal. Flow conservation also applies to entry links of pedestrians, but entering flow is determined by the demand $d_i^{\mathrm{p}}(t)$

$$x_{ij}^{\mathrm{p}}(t+1) = x_{ij}^{\mathrm{p}}(t) - y_{ij}^{\mathrm{p}}(t) + d_i^{\mathrm{p}}(t) \times r_{ij}^{\mathrm{p}}(t) \quad (5)$$

We assume that for entry link $i \in \mathcal{A}_e^{\mathrm{p}}$, $d_i^{\mathrm{p}}(t)$ are independent identically distributed random variables with mean $\overline{d}_i^{\mathrm{p}}$. We further assume $d_i^{\mathrm{p}}(t)$ has maximum value $\tilde{d}_i^{\mathrm{p}}$. Note that Varaiya (2013) did not consider pedestrian access, but we will include the phases that consider pedestrian and vehicle access for the intersection controls. There should be some feasible control that can accommodate pedestrian movements without conflict with vehicles, which will be introduced in the section "Feasible Signal Control Including Pedestrian Access." Furthermore, it is worthy to mention that pedestrians could originate from any node. We provide entry links to make it clear that there are processes or mechanisms to load pedestrian demand into the network. The value of $y_{ij}^{\mathrm{p}}(t)$ is denoted by the following equation:

$$y_{ij}^{\mathrm{p}}(t) = \min\{Q_{ij}^{\mathrm{p}} s_{ij}(t), x_{ij}^{\mathrm{p}}(t)\} \quad (6)$$

Specifically, we assume that pedestrians could move at the capacity of the pedestrian movement from link i to link j if they can move. We use $s_{mb}(t)$ to denote whether crosswalks are activated or not as described in the section "Feasible Signal Control Including Pedestrian Access." Based on the conflict logic, pedestrians can move when they do not have conflicts with vehicles, or when crosswalks are forced to activate for pedestrian cross-movements.

Feasible Signal Control Including Pedestrian Access

The activation of turning movement (i, j) for vehicles and pedestrians is denoted by $s_{ij}(t) \in \{0, 1\}$; $s_{ij}(t) = 1$ means movement (i, j) gets a green light, and $s_{ij}(t) = 0$ means that movement (i, j) gets a red light. Note that when pedestrian movements do not conflict with vehicle movements, pedestrians can still walk across the intersection. Specifically, we define pedestrian cross-movements (walking through the crosswalks) as (m, n), which are a subset of all pedestrian movements (i, j) (including cross-movements and sidewalk-movements).

Let $S_n(t)$ be an intersection matrix for intersection n that include the movement of pedestrians and vehicles. We can define the intersection control sequence $S_n = \{S_n(t), t \in T\}$. Let $\mathcal{S}$ be a set that includes all feasible network control matrices for all intersections, and let $\mathcal{S}_n$ be the set of all feasible intersection matrices for intersection n. We denote the convex hull of all feasible signal control matrices as $Conv(\mathcal{S})$. Because we need to consider pedestrian access, Fig. 3 shows a detailed explanation of feasible signal control including pedestrian access. Pedestrians can walk through crosswalks (crosswalks are activated) when they do not have conflicts with the vehicle movements. Note that in this paper, vehicle movements are determined by signal phase, in contrast with Chen et al. (2020), who used autonomous intersection management, which lacked signal phases.

To consider pedestrian access in the signal control, we define the activation indicator for the pedestrian cross-movement (m, b) as $s_{mb}(t)$. We keep track of pedestrian waiting time by $\phi_{mb}(t)$, as follows:

$$\phi_{mb}(t+1) = \begin{cases} \phi_{mb}(t) + 1 & s_{mb}(t) = 0 \\ 0 & s_{mb}(t) = 1 \end{cases} \quad (7)$$

We set a maximum tolerance time, $\hat{\phi}_{mb}$, which should be tested under different value settings, and we assume this number is exogenous and does not vary with time.

The pedestrian waiting time for cross-movement (m, b) at time step t is denoted as $\phi_{mb}(t)$. When the difference between pedestrian waiting time and maximum tolerance time is larger than zero, $s_{mb}(t)$ is forced to be set to 1 to activate the crosswalk for (m, b). The following equation gives a constant on the activation of pedestrian cross-movement (m, b) based on the tolerance time:

$$(1 - s_{mb}(t))(\phi_{mb}(t) - \hat{\phi}_{mb}) \le 0 \quad (8)$$

In consequence, we are forced to activate the crosswalk at once every $\hat{\phi}_{mb}$ time steps.

When the pedestrian waiting time is less than the maximum tolerance time, $s_{mb}(t)$ could be 0 or 1, but this should depend on whether it conflicts with vehicles. The following equation represents the relationship between vehicles and pedestrians:

$$s_{mb}(t) \le 1 - s_{ij}(t)\alpha_{ij}^{b} \quad (9)$$

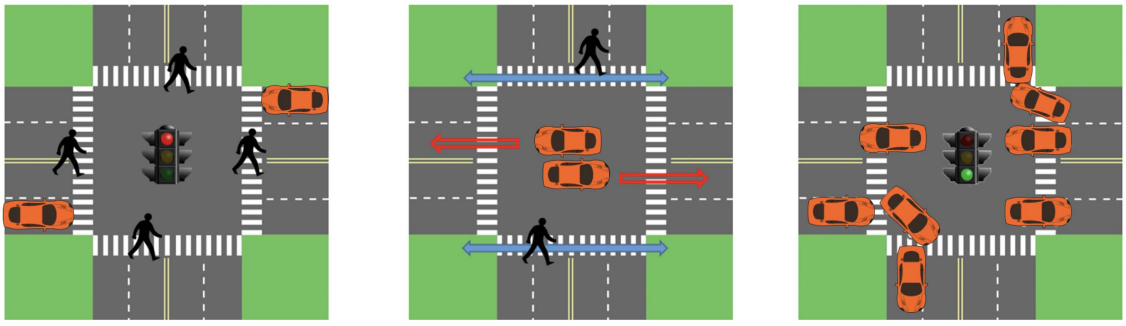

Fig. 3. Traffic signal design with pedestrian access.

J. Transp. Eng., Part A: Systems, 2024, 150(7): 04024028

where $\alpha_{ij}^{b} \in \{0,1\}$ indicates whether vehicle movement (i,j) intersects with crosswalk b.

Overall, we are able to obtain feasible signal control $s_{ij}(t)$ that includes pedestrian movements and vehicle movements. For any given intersection control sequence, the long-term average time used for serving vehicle movement (i,j), including pedestrian access, can be calculated by Eq. (10), which is average signal control. Let $\overline{\mathbf{s}}$ and $\mathbf{s}(t)$ be the vectors of $\overline{s}_{ij}$ and $s_{ij}(t)$, respectively

$$\overline{s}_{ij} = \lim_{T\to\infty} \frac{1}{T} \sum_{t=1}^{T} s_{ij}(t) \tag{10}$$

The convex hull of all feasible signal control matrices $\mathcal{S}$ is given by the following equation:

$$\text{Conv}(\mathcal{S}) = \left\{ \sum_{s\in\mathcal{S}} \lambda_s S | \lambda_s S \le 0, \sum \lambda_s = 1 \right\} \tag{11}$$

Then we can find a set $\mathbb{S} \subset \text{conv}(\mathcal{S})$, which is the set of average control calculated by Eq. (10) where $\mathbf{s}(t)$ satisfies pedestrian access constraints of Eqs. (7)–(9). The category of signal controls includes several types in this research: feasible signal control, average signal control, and Ped-MP. Feasible signal control pertains to traffic signal strategies viable in real-world settings, incorporating both fixed-time and adaptive signal controls. Notably, certain scenarios, like the simultaneous activation of conflicting movements, are deemed infeasible. Conversely, average signal control provides a long-term averaged perspective on the time allocated for movements between links i and j, offering an averaged insight for specific traffic participants but not always guaranteeing feasibility. Ped-MP, designed with pedestrian nuances in mind, stands as a max-pressure signal control under the umbrella of feasible controls. For vehicular traffic between links i and j, it aligns with the average signal control specific to vehicles, whereas for pedestrian traffic, it reflects the average signal control exclusive to their movements. After that, we can give Proposition 1, which is needed for the proof of stability.

Proposition 1: If $\mathbf{s}(t) \in \mathcal{S}$ and $\mathbf{s}(t)$ satisfy pedestrian access constraints (7)–(9), then there exists a $\overline{\mathbf{s}} \in \mathbb{S}$ such that

$$\overline{\mathbf{s}} = \lim_{T\to\infty} \frac{1}{T} \sum_{t=1}^{T} \mathbf{s}(t) \tag{12}$$

Proof: First, we prove that $\overline{\mathbf{s}}$ is in the convex hull of $\mathbb{S}$. For any T, Let $T \times \lambda_{\mathbf{s}}$ be the duration of time steps so that $\mathbf{s}(t) = \mathbf{s}$. Given that $\mathbf{s}(t) \in \mathcal{S}$ and $\mathbf{s}(t)$ satisfy constraints (7)–(9), $\sum_{\mathbf{s}} T\lambda_{\mathbf{s}} = T$. Thus, $\lambda_{\mathbf{s}}$ represents the proportion of time spent in each phase $\mathbf{s}$. The summation across all phases is given by $\sum_{\mathbf{s}} \lambda_{\mathbf{s}} = 1$. Therefore, we define the indicator function as

$$\mathbb{I}(\mathbf{s}(t) = \mathbf{s}) \begin{cases} 1 & \text{if } \mathbf{s}(t) = \mathbf{s} \\ 0 & \text{if } \mathbf{s}(t) \neq \mathbf{s} \end{cases} \tag{13}$$

Then we have

$$\overline{\mathbf{s}} = \lim_{T\to\infty} \frac{1}{T} \sum_{t=1}^{T} \mathbf{s}(t) \tag{14}$$

$$= \lim_{T\to\infty} \frac{1}{T} \sum_{t=1}^{T} \sum_{\mathbf{s}} \mathbb{I}(\mathbf{s}(t) = \mathbf{s})\mathbf{s} \tag{15}$$

$$= \lim_{T\to\infty} \frac{1}{T} \sum_{t=1}^{T} \sum_{\mathbf{s}\in\mathcal{S}} T\lambda_{\mathbf{s}}\mathbf{s} \tag{16}$$

$$= \sum_{\mathbf{s}\in\mathcal{S}} \lambda_{\mathbf{s}}\mathbf{s} \tag{17}$$

Because $\overline{\mathbf{s}} \in \mathbb{S}$, there exists a $\lambda_{\mathbf{s}}$ satisfying $\sum_{\mathbf{s}\in\mathcal{S}} \lambda_{\mathbf{s}} = 1$ such that

$$\overline{\mathbf{s}} = \sum_{\mathbf{s}\in\mathcal{S}} \lambda_{\mathbf{s}}\mathbf{s} \tag{18}$$

Stable Network

Stability means the ability/capacity of network-level signal controls to serve all demand in the transportation network. We should clarify that, while this research seeks to adapt the original MP control to accommodate pedestrian access, the stability definition remains consistent with the concept presented by Varaiya (2013). Specifically, our focus remains on the stability of vehicles rather than pedestrians. However, we do ensure pedestrian movement by activating pedestrian phases after a predetermined duration, denoted as $\hat{\phi}_{mb}$. This approach is further elucidated in the Section "Feasible Signal Control Including Pedestrian Access." Hence, we define the stability of the network mathematically as follows when the signal control included pedestrian access:

Definition 1: The network is strongly stable if the number of vehicles in the network is bounded in expectation, i.e., there exists a $\kappa < \infty$ such that

$$\lim_{T\to\infty} \sup \left\{ \frac{1}{T} \sum_{t=1}^{T} \sum_{(i,j)\in\mathcal{A}^2} \mathbb{E}\{x_{ij}^{\text{v}}(t)\} \right\} \le \kappa \tag{19}$$

Because we can easily find a large demand rate such that no traffic control policy can serve it, it is essential to define the network stable region to prove maximum stability.

Stable Region

MP control aims to stabilize any vehicle demand that could be stabilized by any other signal control. To prove the maximum stability property, we must define analytically the set of vehicle demands that could be stabilized. In reality, the demand for vehicles is stochastic and the stable region is defined in terms of the average demand rates $\overline{\mathbf{d}}^{\text{v}}$ to help us prove the maximum stability. Let $\mathbf{f}^{\text{v}}$ be the average volume of vehicles on link i. For entry links, we have the following relationship:

$$f_i^{\text{v}} = \overline{d}_i^{\text{v}} \tag{20}$$

For internal links of vehicles, f_i^{v} can be determined by conservation of flow, which means the total flow on the downstream link is determined by the aggregation of from all connected upstream flow. This cumulative flow considers the proportion of vehicles transition from each upstream link to the downstream one:

$$f_j^{\text{v}} = \sum_{i\in\mathcal{A}_{\text{v}}} f_i^{\text{v}} \overline{r}_{ij}^{\text{v}} \tag{21}$$

By Proposition 1 of Varaiya (2013), for every demand rate $\overline{\mathbf{d}}^{\text{v}}$ and turning proportions $\overline{\mathbf{r}}^{\text{v}}$, there exists an unique average flow vector $\mathbf{f}^{\text{v}}$. In this study, the network can be stabilized if the average vehicle flow can still be served by some traffic signals considering the access of pedestrian movements. That is, there must exist an average signal activation $\overline{\mathbf{s}} \in \mathbf{S}$. It is crucial to mention that the size of the stable region in this study is smaller compared with Varaiya's (2013) stable region, since the feasible signal phases for vehicles will be restricted by the access of pedestrian's movements by

constraints Eqs. (7)–(9). Specifically, $\overline{\mathbf{s}}$ in Varaiya (2013) are used for vehicles only, but $\overline{\mathbf{s}}$ in this research are forced to close for the activation of pedestrians movement at least every $\hat{\phi}_{mb}$ time steps

$$f_i^{\mathrm{v}}\overline{r}_{ij}^{\mathrm{v}} \le \overline{s}_{ij}Q_{ij}^{\mathrm{v}} \tag{22}$$

where $\overline{s}_{ij}$ can be obtained from Eq. (10), based on some feasible signal control that follows pedestrian access constraints Eqs. (7)–(9).

Let $\mathcal{D}$ be the set of all feasible demand vectors of vehicles $\overline{\mathbf{d}}^{\mathrm{v}}$, which satisfy constraints Eqs. (20)–(22). Let $\mathcal{D}^0$ be the interior of $\mathcal{D}$, where constraint Eq. (22) holds with strict inequality. Then, there exists an $\epsilon > 0$ such that

$$f_i^{\mathrm{v}}\overline{r}_{ij}^{\mathrm{v}} - \overline{s}_{ij}Q_{ij}^{\mathrm{v}} \le -\epsilon \tag{23}$$

Proposition 2: If $\overline{\mathbf{d}} \notin \mathcal{D}^0$, then it is impossible to find a stabilizing control.

Proof: If the network is unstable, the vehicle's movement flow is greater than the traffic signal control policy that can serve. Given that $\overline{\mathbf{d}}^{\mathrm{v}}$, $\forall \overline{s}_{ij} \in \mathcal{S}$, there exists a $\theta > 0$ and at least one turning movement (i, j) satisfying $f_j^{\mathrm{v}}\overline{r}_{ij}^{\mathrm{v}} \ge \overline{s}_{ij}Q_{ij}^{\mathrm{v}} + \theta$.

Based on Eq. (1), we have

$$x_{ij}^{\mathrm{v}}(t+1) - x_{ij}^{\mathrm{v}}(t) = \sum_{(i,j,h)\in(\mathcal{A}^{\mathrm{v}})^3} y_{hi}^{\mathrm{v}}(t) \times r_{ij}^{\mathrm{v}}(t) - y_{ij}^{\mathrm{v}}(t) \tag{24}$$

Based on Eq. (24), we can obtain the following relationship:

$$\mathbb{E}\left[\sum_{t=0}^{\tau-1}\sum_{(i,j)\in\mathcal{A}^{\mathrm{v}2}}(x_{ij}^{\mathrm{v}}(t+1) - x_{ij}^{\mathrm{v}}(t))\right] = \mathbb{E}\left[\sum_{(i,j)\in\mathcal{A}^{\mathrm{v}2}}(x_{ij}^{\mathrm{v}}(\tau) - x_{ij}^{\mathrm{v}}(0))\right] \tag{25}$$

$$= \mathbb{E}\left[\sum_{t=0}^{\tau-1}\sum_{(i,j,h)\in(\mathcal{A}^{\mathrm{v}})^3}(y_{hi}^{\mathrm{v}}(t)r_{ij}^{\mathrm{v}}(t) - y_{ij}^{\mathrm{v}}(t))\right] \tag{26}$$

$$= \mathbb{E}\left[\sum_{((i,j)\in\mathcal{A}^{\mathrm{v}2}}(f_j^{\mathrm{v}}\overline{r}_{ij}^{\mathrm{v}} - \overline{s}_{ij}Q_{ij}^{\mathrm{v}})\right] \tag{27}$$

$$\ge \mathbb{E}[\tau\theta)] = \tau\theta \tag{28}$$

Moving $x_{ij}^{\mathrm{v}}(0)$ to the right hand side, we obtain

$$\mathbb{E}\left[\sum_{(i,j)\in\mathcal{A}^{\mathrm{v}2}} x_{ij}^{\mathrm{v}}(\tau)\right] \ge \theta\tau + \mathbb{E}\left[\sum_{(i,j)\in\mathcal{A}^{\mathrm{v}2}} x_{ij}^{\mathrm{v}}(0)\right] \tag{29}$$

or equivalently

$$\mathbb{E}[|\mathbf{x}^{\mathrm{v}}(\tau)|] \ge \theta\tau + \mathbb{E}[|\mathbf{x}^{\mathrm{v}}(0)|] \tag{30}$$

From Eq. (30), we obtain

$$\begin{aligned}\lim_{T\to\infty}\mathbb{E}\left[\frac{1}{T}\sum_{t=1}^{T}|\mathbf{x}^{\mathrm{v}}(t)|\right] &\ge \lim_{T\to\infty}\mathbb{E}\left[\frac{1}{T}\sum_{t=1}^{T}[\theta t + \mathbb{E}[|\mathbf{x}^{\mathrm{v}}(0)|]]\right] \\ &= \lim_{T\to\infty}\mathbb{E}\left[\frac{1}{T}\sum_{t=1}^{T}(\theta t)\right] + \lim_{T\to\infty}\mathbb{E}\left[\frac{1}{T}\sum_{t=1}^{T}[|\mathbf{x}^{\mathrm{v}}(0)|]\right] = \infty\end{aligned} \tag{31}$$

which violates Eq. (19).

Stability Analysis Based on Average Signal Control

Now, we need to prove that the average signal control, including pedestrian access, will stabilize any demand vectors $\overline{\mathbf{d}} \in \mathcal{D}^0$. It is a prerequisite for the MP control to achieve maximum stability, because, if there exists no average signal control including pedestrian access, that can stabilize any demand vectors $\overline{\mathbf{d}} \in \mathcal{D}^0$, MP control cannot stabilize the network either. In addition, any demand $\overline{\mathbf{d}} \notin \mathcal{D}$ cannot be stabilized by Proposition 2, and this essentially proves that the average signal control can achieve stability. The only excluded demand is on the boundary of $\mathcal{D}$, for which the Markov chain can be shown to be null recurrent but not positive recurrent. Note that we only consider the stability of vehicles because pedestrians can move once the tolerance time is reached.

Lemma 1: When $\overline{\mathbf{d}} \in \mathcal{D}^0$, there exists a Lyapunov function $\nu(t) \ge 0$ and constants $\kappa < \infty$, $\epsilon > 0$ such that

$$\mathbb{E}[\nu(t+1) - \nu(t)|\mathbf{x}(t)] \le \kappa - \epsilon|\mathbf{x}(t)| \tag{32}$$

Proof: To calculate the queue length at time $t+1$, we apply the vehicle queueing models shown in Eqs. (1)–(6). Then, let $\delta_{ij}(t)$ be the difference of the queueing length of vehicles between time steps t and time steps $t+1$

$$\begin{aligned}\delta_{ij}(t) &= x_{ij}^{\mathrm{v}}(t+1) - x_{ij}^{\mathrm{v}}(t) \\ &= -\min\{Q_{ij}^{\mathrm{v}}s_{ij}(t), x_{ij}^{\mathrm{v}}(t)\} \\ &\quad + \sum_{h\in\mathcal{A}_i^-}\min\{Q_{hi}^{\mathrm{v}}s_{ij}(t), x_{hi}^{\mathrm{v}}(t)\} \times r_{ij}^{\mathrm{v}}(t) \quad \forall\ i \in \mathcal{A}_{\mathrm{i}}, j \in \Gamma_i^+\end{aligned} \tag{33}$$

$$\begin{aligned}\delta_{ij}(t) &= x_{ij}^{\mathrm{v}}(t+1) - x_{ij}^{\mathrm{v}}(t) \\ &= -\min\{Q_{ij}^{\mathrm{v}}s_{ij}(t), x_{ij}^{\mathrm{v}}(t)\} + d_i^{\mathrm{v}}(t) \times r_{ij}^{\mathrm{v}}(t) \quad \forall\ i \in \mathcal{A}_{\mathrm{e}}, j \in \Gamma_i^+\end{aligned} \tag{34}$$

Let $\mathbf{x}^{\mathrm{v}}(t)$ be the matrix including all queue length of private vehicles. Hence, we consider the Lyapunov function $\nu(t)$ as follows:

$$\nu(t) = |\mathbf{x}^{\mathrm{v}}(t)|^2 = \sum_{(i,j)\in\mathcal{A}^2}(x_{ij}^{\mathrm{v}}(t))^2 \tag{35}$$

Then, we expand the difference $\nu_1(t+1) - \nu_1(t)$ as follows:

$$\begin{aligned}\nu(t+1) - \nu(t) &= |\mathbf{x}^{\mathrm{v}}(t+1)|^2 - |\mathbf{x}^{\mathrm{v}}(t)|^2 \\ &= |\mathbf{x}^{\mathrm{v}}(t) + \boldsymbol{\delta}(t)|^2 - |\mathbf{x}^{\mathrm{v}}(t)|^2 \\ &= 2\mathbf{x}^{\mathrm{v}}(t)^{\mathrm{T}}\boldsymbol{\delta}(t) + |\boldsymbol{\delta}(t)|^2\end{aligned} \tag{36}$$

The first term of Eq. (36) can be rewritten as

$$\begin{aligned}2\mathbf{x}^{\mathrm{v}}(t)^{\mathrm{T}}\boldsymbol{\delta}(t) &= -2x_{ij}^{\mathrm{v}}(t)\sum_{i\in\mathcal{A}}\sum_{j\in\Gamma_i^+}\min\{Q_{ij}^{\mathrm{v}}s_{ij}(t), x_{ij}^{\mathrm{v}}(t)\} \\ &\quad + 2\sum_{h\in\Gamma_i^-}\sum_{i\in\mathcal{A}}\sum_{j\in\Gamma_i^+}x_{ij}^{\mathrm{v}}(t)\min\{Q_{hi}^{\mathrm{v}}s_{hi}(t), x_{hi}^{\mathrm{v}}(t)\}r_{ij}^{\mathrm{v}}(t) \\ &\quad + 2\sum_{i\in\mathcal{A}_{\mathrm{e}}}\sum_{j\in\Gamma_i^+}(-\min\{Q_{ij}^{\mathrm{v}}s_{ij}(t), x_{ij}^{\mathrm{v}}(t)\} + d_i^{\mathrm{v}}(t) \times r_{ij}^{\mathrm{v}}(t))\end{aligned} \tag{37}$$

$$\begin{aligned}&= 2\sum_{i\in\mathcal{A}_{\mathrm{i}}\cup\mathcal{A}_{\mathrm{e}}}\sum_{j\in\Gamma_i^+}\min\{Q_{ij}^{\mathrm{v}}s_{ij}(t), x_{ij}^{\mathrm{v}}(t)\}\left(-x_{ij}^{\mathrm{v}}(t) + \sum_{k\in\Gamma_i^+}r_{jk}^{\mathrm{v}}(t)x_{jk}^{\mathrm{v}}(t)\right) \\ &\quad + 2\sum_{i\in\mathcal{A}_{\mathrm{e}}}\sum_{j\in\Gamma_i^+}d_i^{\mathrm{v}}(t) \times r_{ij}^{\mathrm{v}}(t) \times x_{ij}^{\mathrm{v}}(t)\end{aligned} \tag{38}$$

We replace the turning proportion $r_{ij}^{\mathrm{v}}(t)$ with average value $\overline{r}_{ij}^{\mathrm{v}}$, since

$$\lim_{T\to\infty}\frac{1}{T}\sum_{t=1}^{T}\sum_{(i,j)\in\mathcal{A}^2} r_{ij}^{\mathrm{v}}(t)=\sum_{i,j\in\mathcal{A}}\overline{r}_{ij}^{\mathrm{v}}$$

and $r_{ij}^{\mathrm{v}}(t)$ is a random variable. Therefore, we have the following equation:

$$\begin{aligned}
&\mathbb{E}[\mathbf{x}^{\mathrm{v}}(t)^{\mathrm{T}}\boldsymbol{\delta}(t)|\mathbf{x}^{\mathrm{v}}(t)]\\
&\quad=\sum_{i\in\mathcal{A}_{\mathrm{i}}\cup\mathcal{A}_{\mathrm{e}}}\sum_{j\in\Gamma_i^+}\mathbb{E}[\min\{Q_{ij}^{\mathrm{v}}s_{ij}(t),x_{ij}^{\mathrm{v}}(t)\}\times(-x_{ij}^{\mathrm{v}}(t))|\mathbf{x}^{\mathrm{v}}(t)]\\
&\qquad+\sum_{i\in\mathcal{A}_{\mathrm{i}}\cup\mathcal{A}_{\mathrm{e}}}\sum_{j\in\Gamma_i^+}\mathbb{E}[\min\{Q_{ij}^{\mathrm{v}}s_{ij}(t),x_{ij}^{\mathrm{v}}(t)\}|\mathbf{x}^{\mathrm{v}}(t)]\\
&\qquad\times\left(\sum_{k\in\Gamma_i^+}\overline{r}_{jk}^{\mathrm{v}}x_{jk}^{\mathrm{v}}(t)\right)+\sum_{i\in\mathcal{A}_{\mathrm{e}}}\sum_{j\in\Gamma_i^+}\mathbb{E}[d_i^{\mathrm{v}}(t)\overline{r}_{ij}^{\mathrm{v}}x_{ij}^{\mathrm{v}}(t)|\mathbf{x}^{\mathrm{v}}(t)] \qquad (39)
\end{aligned}$$

Then, we obtain

$$\begin{aligned}
&\mathbb{E}[\mathbf{x}^{\mathrm{v}}(t)^{\mathrm{T}}\boldsymbol{\delta}(t)|\mathbf{x}^{\mathrm{v}}(t)]\\
&\quad=\sum_{i\in\mathcal{A}_{\mathrm{i}}\cup\mathcal{A}_{\mathrm{e}}}\mathbb{E}[\min\{Q_{ij}^{\mathrm{v}}s_{ij}(t),x_{ij}^{\mathrm{v}}(t)\}|\mathbf{x}^{\mathrm{v}}(t)]\\
&\qquad\times\left(-x_{ij}^{\mathrm{v}}(t)+\sum_{k\in\Gamma_i^+}\overline{r}_{jk}^{\mathrm{v}}x_{jk}^{\mathrm{v}}(t)\right)+\sum_{i\in\mathcal{A}_{\mathrm{e}}}\overline{d}_i^{\mathrm{v}}\overline{r}_{ij}^{\mathrm{v}}x_{ij}^{\mathrm{v}}(t) \qquad (40)
\end{aligned}$$

For the last term of Eq. (40), $\sum_{i\in\mathcal{A}_{\mathrm{e}}}\overline{d}_i^{\mathrm{v}}\overline{r}_{ij}^{\mathrm{v}}x_{ij}^{\mathrm{v}}(t)$, we have

$$\sum_{i\in\mathcal{A}_{\mathrm{e}}}\overline{d}_i^{\mathrm{v}}\overline{r}_{ij}^{\mathrm{v}}x_{ij}^{\mathrm{v}}(t)=\sum_{i\in\mathcal{A}_{\mathrm{e}}}f_i^{\mathrm{v}}\overline{r}_{ij}^{\mathrm{v}}x_{ij}^{\mathrm{v}}(t)=\sum_{i\in\mathcal{A}_{\mathrm{e}}}f_{ij}^{\mathrm{v}}x_{ij}^{\mathrm{v}}(t) \qquad (41)$$

$$=\sum_{i\in\mathcal{A}_{\mathrm{i}}\cup\mathcal{A}_{\mathrm{e}}}f_i^{\mathrm{v}}\overline{r}_{ij}^{\mathrm{v}}x_{ij}^{\mathrm{v}}(t)-\sum_{j\in\mathcal{A}_{\mathrm{i}}}f_j^{\mathrm{v}}\overline{r}_{jk}^{\mathrm{v}}x_{jk}^{\mathrm{v}}(t) \qquad (42)$$

$$=\sum_{i\in\mathcal{A}_{\mathrm{i}}\cup\mathcal{A}_{\mathrm{e}}}f_i^{\mathrm{v}}\overline{r}_{ij}^{\mathrm{v}}x_{ij}^{\mathrm{v}}(t)-\sum_{j\in\Gamma_i^+}\left[\sum_{i\in\mathcal{A}_{\mathrm{i}}\cup\mathcal{A}_{\mathrm{e}}}f_i^{\mathrm{v}}\overline{r}_{ij}^{\mathrm{v}}\right]\sum_{K}\overline{r}_{jk}^{\mathrm{v}}x_{jk}^{\mathrm{v}}(t) \qquad (43)$$

$$=\sum_{i\in\mathcal{A}_{\mathrm{i}}\cup\mathcal{A}_{\mathrm{e}}}f_i^{\mathrm{v}}\overline{r}_{ij}^{\mathrm{v}}\left(x_{ij}^{\mathrm{v}}(t)-\sum_{k}\overline{r}_{jk}^{\mathrm{v}}x_{jk}^{\mathrm{v}}(t)\right) \qquad (44)$$

By Proposition 1, there exists some $\overline{\mathbf{s}}\in Conv(\mathcal{S})$ such that $\mathbb{E}[s_{ij}(t)]=\overline{s}_{ij}$. Then, we have

$$\begin{aligned}
&\mathbb{E}[\mathbf{x}^{\mathrm{v}}(t)^{\mathrm{T}}\boldsymbol{\delta}(t)|\mathbf{x}^{\mathrm{v}}(t)]\\
&\quad=\sum_{i\in\mathcal{A}_{\mathrm{i}}\cup\mathcal{A}_{\mathrm{e}}}(f_i^{\mathrm{v}}\overline{r}_{ij}^{\mathrm{v}}-\mathbb{E}[\min\{Q_{ij}^{\mathrm{v}}s_{ij}(t),\mathbf{x}^{\mathrm{v}}(t)\}|\mathbf{x}^{\mathrm{v}}(t)])\\
&\qquad\times\left(x_{ij}^{\mathrm{v}}(t)-\sum_{k\in\Gamma_j^+}\overline{r}_{jk}^{\mathrm{v}}x_{jk}^{\mathrm{v}}(t)\right) \qquad (45)
\end{aligned}$$

$$\begin{aligned}
&=\sum_{i\in\mathcal{A}_{\mathrm{i}}\cup\mathcal{A}_{\mathrm{e}}}(f_i^{\mathrm{v}}\overline{r}_{ij}^{\mathrm{v}}-\overline{s}_{ij}Q_{ij}^{\mathrm{v}})\left(x_{ij}^{\mathrm{v}}(t)-\sum_{k\in\Gamma_j^+}\overline{r}_{jk}^{\mathrm{v}}x_{jk}^{\mathrm{v}}(t)\right)\\
&\quad+\sum_{i\in\mathcal{A}_{\mathrm{i}}\cup\mathcal{A}_{\mathrm{e}}}(\overline{s}_{ij}Q_{ij}^{\mathrm{v}}-\mathbb{E}[\min\{Q_{ij}^{\mathrm{v}}s_{ij}(t),x_{ij}^{\mathrm{v}}(t)\}|\mathbf{x}^{\mathrm{v}}(t)])\\
&\qquad\times\left(x_{ij}^{\mathrm{v}}(t)-\sum_{k\in\Gamma_j^+}\overline{r}_{jk}^{\mathrm{v}}x_{jk}^{\mathrm{v}}(t)\right) \qquad (46)
\end{aligned}$$

For the second term of Eq. (46), if $x_{ij}^{\mathrm{v}}(t)\geq Q_{ij}^{\mathrm{v}}$, we have $\mathbb{E}[\min\{Q_{ij}^{\mathrm{v}}s_{ij}(t),x_{ij}^{\mathrm{v}}(t)\}|\mathbf{x}^{\mathrm{v}}(t)]=Q_{ij}^{\mathrm{v}}\overline{s}_{ij}$. Therefore, the second term of Eq. (46) equals zero. If $x_{ij}^{\mathrm{v}}(t)<Q_{ij}^{\mathrm{v}}$, then we have $\mathbb{E}[\min\{Q_{ij}^{\mathrm{v}}s_{ij}(t),x_{ij}^{\mathrm{v}}(t)\}|\mathbf{x}^{\mathrm{v}}(t)]=\mathbb{E}[x_{ij}^{\mathrm{v}}(t)|\mathbf{x}^{\mathrm{v}}(t)]$, which results in

$$\begin{aligned}
&\sum_{i\in\mathcal{A}_{\mathrm{i}}\cup\mathcal{A}_{\mathrm{e}}}(\overline{s}_{ij}Q_{ij}^{\mathrm{v}}-\mathbb{E}[x_{ij}^{\mathrm{v}}(t)|\mathbf{x}^{\mathrm{v}}(t)])\left(x_{ij}^{\mathrm{v}}(t)-\sum_{k\in\Gamma_j^+}\overline{r}_{jk}^{\mathrm{v}}x_{jk}^{\mathrm{v}}(t)\right)\\
&\quad\leq\sum_{i\in\mathcal{A}_{\mathrm{i}}\cup\mathcal{A}_{\mathrm{e}}}\overline{s}_{ij}Q_{ij}^{\mathrm{v}}x_{ij}^{\mathrm{v}}(t)\leq\sum_{i\in\mathcal{A}_{\mathrm{i}}\cup\mathcal{A}_{\mathrm{e}}}(Q_{ij}^{\mathrm{v}})^2 \qquad (47)
\end{aligned}$$

Therefore, the second term of Eq. (46) equals zero or is bounded by $\sum_{i\in\mathcal{A}_{\mathrm{i}}\cup\mathcal{A}_{\mathrm{e}}}(Q_{ij}^{\mathrm{v}})^2$. Moving on, we focus on the first term of Eq. (46). Based on the inequality Eq. (23), we have

$$\begin{aligned}
&\sum_{i\in\mathcal{A}_{\mathrm{i}}\cup\mathcal{A}_{\mathrm{e}}}(f_i^{\mathrm{v}}\overline{r}_{ij}^{\mathrm{v}}-\overline{s}_{ij}Q_{ij}^{\mathrm{v}})\left(x_{ij}^{\mathrm{v}}(t)-\sum_{k\in\Gamma_j^+}\overline{r}_{jk}^{\mathrm{v}}x_{jk}^{\mathrm{v}}(t)\right)\\
&\quad\leq\sum_{i\in\mathcal{A}_{\mathrm{i}}\cup\mathcal{A}_{\mathrm{e}}}(f_i^{\mathrm{v}}\overline{r}_{ij}^{\mathrm{v}}-\overline{s}_{ij}Q_{ij}^{\mathrm{v}})(x_{ij}^{\mathrm{v}}(t))\leq-\epsilon|\mathbf{x}^{\mathrm{v}}(t)| \qquad (48)
\end{aligned}$$

Eq. (32) satisfies the following relationship based on Eqs. (47) and (48). For $\delta_{ij}(t)$

$$\begin{aligned}
|\delta_{ij}(t)|=&\Big|-\min\{Q_{ij}^{\mathrm{v}}s_{ij}(t),x_{ij}^{\mathrm{v}}(t)\}\\
&+\sum_{h\in\mathcal{A}_i^-}\min\{Q_{hi}^{\mathrm{v}}s_{ij}(t),x_{hi}^{\mathrm{v}}(t)\}\times r_{ij}^{\mathrm{v}}(t)\Big|\\
&\forall\ i\in\mathcal{A}_{\mathrm{i}},j\in\Gamma_i^+ \qquad (49)
\end{aligned}$$

$$\leq\max\left\{Q_{ij}^{\mathrm{v}},\sum_{h\in\mathcal{A}_i^-}Q_{ij}^{\mathrm{v}}\right\} \qquad (50)$$

Let $\hat{d}_{ij}$ be the maximum value of demand. Then, we have

$$|\delta_{ij}(t)|=|-\min\{Q_{ij}^{\mathrm{v}}s_{ij}(t),x_{ij}^{\mathrm{v}}(t)\}+d_i^{\mathrm{v}}(t)\times r_{ij}^{\mathrm{v}}|\leq\max\{Q_{ij}^{\mathrm{v}},\hat{d}_{ij}\}\quad\forall\ i\in\mathcal{A}_{\mathrm{e}},j\in\Gamma_i^+ \qquad (51)$$

Define ψ as the maximum value among Q_{ij}^{v}, $\sum_{h\in\mathcal{A}_i^-}Q_{ij}^{\mathrm{v}}$, and $\hat{d}_{ij}$, that is

$$\psi=\max\left\{Q_{ij}^{\mathrm{v}},\sum_{h\in\mathcal{A}_i^-}Q_{ij}^{\mathrm{v}},\hat{d}_{ij}\right\} \qquad (52)$$

Because the total movement of private vehicles is $\mathcal{M}$, we have the following inequality:

$$|\delta_{ij}(t)|^2\leq\mathrm{M}\times\psi^2 \qquad (53)$$

From Eqs. (48) and (53), we have

$$\begin{aligned}
|\mathbf{x}^{\mathrm{v}}(t+1)|^2-|\mathbf{x}^{\mathrm{v}}(t)|^2&=2\mathbf{x}^{\mathrm{v}}(t)^{\mathrm{T}}\boldsymbol{\delta}(t)+|\boldsymbol{\delta}(t)|^2\\
&\leq 2\left(\sum_{i\in\mathcal{A}_{\mathrm{i}}\cup\mathcal{A}_{\mathrm{e}}}(Q_{ij}^{\mathrm{v}})^2-\epsilon|\mathbf{x}^{\mathrm{v}}(t)|\right)+\mathrm{M}\psi^2 \qquad (54)\\
&=\kappa-\epsilon|\mathbf{x}^{\mathrm{v}}(t)| \qquad (55)
\end{aligned}$$

where $\kappa=2\sum_{i\in\mathcal{A}_{\mathrm{i}}\cup\mathcal{A}_{\mathrm{e}}}(Q_{ij}^{\mathrm{v}})^2+\mathrm{M}\psi^2$.

Based on the above procedure, we find that we do know the lower and upper bounds of $\overline{s}_{ij}$ to prove stability. However, we need the long-time average signal activated time $\overline{s}_{ij}$ used for serving turning movement (i,j) while providing pedestrian access.

Proposition 3: When the average signal $\overline{s}_{ij}$, which is constrained by the stable region definition, is used, and there exists $\overline{\mathbf{d}}^{\mathrm{v}} \in \mathcal{D}^0$, the transportation network is stable.

Proof: Inequality (32) holds from Lemma 1. Taking expectations and summing over $t = 1, \ldots, T$ gives the following inequality:

$$\mathbb{E}[\nu(T+1) - \nu(1)|\mathbf{x}^{\mathrm{v}}(t)] \leq \kappa T - \epsilon \sum_{t=1}^{T} |\mathbf{x}^{\mathrm{P}}(t)| \tag{56}$$

Then, we have

$$\epsilon \frac{1}{T} \sum_{t=1}^{T} \mathbb{E}[|\mathbf{x}^{\mathrm{v}}(t)|] \leq \kappa - \frac{1}{T}\mathbb{E}[\nu(T+1)] + \frac{1}{T}\mathbb{E}[\nu(1)]$$
$$\leq \kappa + \frac{1}{T}\mathbb{E}[\nu(1)] \tag{57}$$

which implies that Definition 1 is satisfied.

Moreover, we need to mention that stability is not impacted by the initial condition. Let us move ϵ in to the right-hand side and take the limit as T goes to infinity. Then, the $(1/T)\mathbb{E}[\nu(1)]$ term equals zero, which yields the following inequality:

$$\lim_{T\to\infty} \frac{1}{T} \sum_{t=1}^{T} \mathbb{E}[|\mathbf{x}^{\mathrm{v}}(t)|] \leq \frac{\kappa}{\epsilon} \tag{58}$$

MP Control Policy

MP Control Policy Considering Pedestrian Access

Now, we reach MP control. We have established that average signal controls accommodating pedestrian access can stabilize the network. Building on this foundation, we aim to demonstrate that the max-pressure (MP) control strategy, when it factors in pedestrian crossings, can also attain maximum stability. This study modifies the original MP control policy of Varaiya (2013) to create the pedestrian-friendly max-pressure signal control policy, Ped-MP. The weight calculation is the same as previous papers (Varaiya 2013; Chen et al. 2020; Levin et al. 2019, 2020)

$$w_{ij}^{\mathrm{v}}(t) = x_{ij}^{\mathrm{v}}(t) - \sum_{k\in\Gamma_j^+} r_{jk}^{\mathrm{v}}(t) x_{jk}^{\mathrm{v}}(t) \tag{59}$$

After we calculate the weight for each movement, a mixed-integer linear program is used to calculate the intersection control. In this program, we use α_{ij}^b to indicate whether the vehicles' movements have conflicts with pedestrians. The capacity of conflict region c is Q_c, which is determined by the capacities of turning movements, $Q_c = \max_{(i,j)|c\in C_{ij}}\{Q_{ij}\}$.

The modified MP control policy considering pedestrian access tries to maximize the total pressure of vehicles. Here, $s_{ij}^*(t)$ denotes the MP signal control at intersection n in the transportation network considering pedestrian access, which is

$$s_{ij}^*(t) = \mathrm{argmax}_{s\in\mathcal{S}}\left[\sum_{(i,j)\in\mathcal{M}} s_{ij}(t) Q_{ij}^{\mathrm{v}} w_{ij}^{\mathrm{v}}(t)\right] \tag{60}$$

which should obey constraints Eqs. (61*a*)–(61*j*). We include pedestrian access constraints Eqs. (8) and (9) in this part as constraints Eqs. (61*b*) and (61*c*) for the convenience of readers. To be specific, constraint Eq. (61*b*) indicates the MP control will consider the pedestrians' waiting time. The maximum tolerance time, which is $\hat{\phi}_{mb}$ in the simulation, should be tested under different value settings, and we assume this number should not change by time (input parameter for simulation). However, a short tolerance time will reduce the stable region of a vehicle significantly, so it should depend on the demand of vehicles and pedestrians in the real world. The pedestrians' waiting time for cross-movement (m, b) at time step t is denoted as $\phi_{mb}(t)$ (section "Feasible Signal Control Including Pedestrian Access"). When the difference between the pedestrians' waiting time and the maximum tolerance time is large than zero, $s_{mb}(t)$ is forced to equal 1, which means, when the pedestrians have been waiting for a long time, we activate the movement for the pedestrians. When the difference between pedestrians' waiting time and the maximum tolerance time is less than or equal to zero, $s_{mb}(t)$ could be 0 or 1, but this should depend on whether it conflicts with vehicles or not. Constraint Eq. (61*c*) represents the relationship with vehicle movements and pedestrians' movements, where $\alpha_{ij}^b \in \{0, 1\}$ indicates whether vehicle movements (i, j) intersect with crosswalk b. For instance, when vehicle movement (i, j) is activated, if it intersects with crosswalk b, then $s_{mb}(t)$ is forced to be zero. However, if movement (i, j) does not conflict with crosswalk b, then $s_{mb}(t)$ could be 0 or 1. Constraint Eq. (61*d*) corresponds with Eq. (3), stipulating that the number of vehicles moving from link i to link j equates to the lesser of two values: the product of the movement's capacity and the signal control indicator, or the queue length for the movement. This ensures that vehicle flow does not exceed the designated capacity or available space in the queue. Constraint Eq. (61*f*) indicates the pedestrian flow from m to b is not permitted unless $s_{mb}(t) = 1$

$$\max \sum_{(i,j)\in\mathcal{M}^2} s_{ij}(t) Q_{ij}^{\mathrm{v}} w_{ij}^{\mathrm{v}}(t) \tag{61a}$$

$$\text{s.t. } (1 - s_{mb}(t))(\phi_{mb}(t) - \hat{\phi}_{mb}) \leq 0 \quad \forall\ b \in \mathcal{Z}, , m \in \Gamma_i^- \tag{61b}$$

$$s_{mb}(t) \leq 1 - s_{ij}(t)\alpha_{ij}^b \quad \forall\ (i,j) \in \mathcal{M}, \quad \forall\ b \in \mathcal{Z}, , m \in \Gamma_i^- \tag{61c}$$

$$\sum_{(i,j)\in\mathcal{M}} y_{ij}^{\mathrm{v}}(t)(1 - \alpha_{ij}^b) \leq Q_{\mathrm{c}} \quad \forall\ (i,j) \in \mathcal{M}, \quad \forall\ b \in \mathcal{Z},$$
$$\forall\ c \in \mathcal{C}, , m \in \Gamma_i^- \tag{61d}$$

$$y_{ij}^{\mathrm{v}}(t) = \min\{Q_{ij}^{\mathrm{v}} s_{ij}(t), x_{ij}^{\mathrm{v}}(t)\} \quad \forall\ (i,j) \in \mathcal{M} \tag{61e}$$

$$y_{mb}^{\mathrm{p}}(t) \in \{0, x_{mb}^{\mathrm{p}}(t)\} \quad \forall\ (b) \in \mathcal{Z}, , m \in \Gamma_i^- \tag{61f}$$

$$s_{ij}(t) \in \{0, 1\} \quad \forall\ (i,j) \in \mathcal{M} \tag{61g}$$

$$s_{mb}(t) \in \{0, 1\} \quad \forall\ (b) \in \mathcal{Z}, m \in \Gamma_i^- \tag{61h}$$

$$\alpha_{ij}^b \in \{0, 1\} \quad \forall\ (i,j) \in \mathcal{M}, \quad \forall\ b \in \mathcal{Z}, , m \in \Gamma_i^- \tag{61i}$$

$$x_{ij}^{\mathrm{v}}(t), x_{mb}^{\mathrm{p}}(t) \geq 0 \quad \forall\ (i,j) \in \mathcal{M}, \quad \forall\ b \in \mathcal{Z}, m \in \Gamma_i^- \tag{61j}$$

Lemma 2: If the modified max-pressure signal control policy, Ped-MP, is used and $\overline{\mathbf{d}} \in \mathcal{D}^0$, then we have the following inequality with average signal control $\overline{s}_{ij}$ including pedestrian access:

$$\mathbb{E}\left[\sum_{(i,j)\in\mathcal{M}^2} s_{ij}^*(t) Q_{ij}^{\mathrm{v}} w_{ij}^{\mathrm{v}}(t) | \mathbf{x}^{\mathrm{v}}(t)\right] \geq \mathbb{E}\left[\sum_{(i,j)\in\mathcal{M}^2} \overline{s}_{ij} Q_{ij}^{\mathrm{v}} w_{ij}^{\mathrm{v}}(t) | \mathbf{x}^{\mathrm{v}}(t)\right] \tag{62}$$

Proof: First, we have the following inequality based on definition of MP control. Given that $s_{ij}^*(t)$, $s_{ij}(t)$ are some feasible signal controls and satisfy constraints Eqs. (61*b*) and (61*c*), and $s_{ij}^*(t)$ maximizes objective Eq. (61*a*), we have

$$\sum_{(i,j)\in\mathcal{M}^2} s_{ij}^*(t) Q_{ij}^{\mathrm{v}} w_{ij}^{\mathrm{v}}(t) \geq \sum_{(i,j)\in\mathcal{M}^2} s_{ij}(t) Q_{ij}^{\mathrm{v}} w_{ij}^{\mathrm{v}}(t) \tag{63}$$

Then, calculating the expected value of the above equation when given the private vehicle queue length $\mathbf{x}^{\mathrm{v}}(t)$, we have

$$\mathbb{E}\left[\sum_{(i,j)\in\mathcal{M}^2} s_{ij}^*(t) Q_{ij}^{\mathrm{v}} w_{ij}^{\mathrm{v}}(t) | \mathbf{x}^{\mathrm{v}}(t)\right] \geq \mathbb{E}\left[\sum_{(i,j)\in\mathcal{M}^2} s_{ij}(t) Q_{ij}^{\mathrm{v}} w_{ij}^{\mathrm{v}}(t) | \mathbf{x}^{\mathrm{v}}(t)\right] \tag{64}$$

Because $s_{ij}^*(t) = \operatorname{argmax}_{s\in\mathcal{S}} \sum_{(i,j)\in\mathcal{M}^2} s_{ij}(t) Q_{ij}^{\mathrm{v}} w_{ij}^{\mathrm{v}}(t)$ based on Eq. (10) where $s_{ij}(t)$ satisfies constraint Eqs. (61*b*) and (61*c*), we rewrite Eq. (62) as

$$\mathbb{E}\left[\sum_{(i,j)\in\mathcal{M}^2} s_{ij}^*(t) Q_{ij}^{\mathrm{v}} w_{ij}^{\mathrm{v}}(t) | \mathbf{x}^{\mathrm{v}}(t)\right] \geq \mathbb{E}\left[\sum_{(i,j)\in\mathcal{M}^2} \overline{s}_{ij} Q_{ij}^{\mathrm{v}} w_{ij}^{\mathrm{v}}(t) | \mathbf{x}^{\mathrm{v}}(t)\right] \tag{65}$$

Stability Analysis Based on Ped-MP

Lemma 3: If the modified max-pressure control policy, Ped-MP, is used, and $\overline{\mathbf{d}} \in \mathcal{D}^0$, there exists a Lyapunov function $\nu(t) \geq 0$ and constants $\kappa > 0$, $\epsilon > 0$ such that

$$\mathbb{E}[\nu(t+1) - \nu(t) | \mathbf{x}^{\mathrm{v}}(t)] \leq \kappa - \eta |\mathbf{x}^{\mathrm{v}}(t)| \tag{66}$$

Proof: Based on Eqs. (10)–(40) and the definition of pressure term Eq. (59), we obtain

$$\begin{aligned}\mathbb{E}[\mathbf{x}^{\mathrm{v}}(t)^{\mathrm{T}} \boldsymbol{\delta}(t) | \mathbf{x}^{\mathrm{v}}(t)] = & \sum_{i\in\mathcal{A}_{\mathrm{i}}\cup\mathcal{A}_{\mathrm{e}}} \mathbb{E}[\min\{Q_{ij}^{\mathrm{v}} s_{ij}(t), x_{ij}^{\mathrm{v}}(t)\} | \mathbf{x}^{\mathrm{v}}(t)] \\ & \times (-w_{ij}^{\mathrm{v}}(t)) + \sum_{i\in\mathcal{A}_{\mathrm{e}}} \overline{d}_i^{\mathrm{v}} \overline{r}_{ij}^{\mathrm{v}} x_{ij}^{\mathrm{v}}(t)\end{aligned} \tag{67}$$

The last term of Eq. (67) can be rewritten as follows based on Eqs. (20), (21), and (59), as follows:

$$\sum_{i\in\mathcal{A}_{\mathrm{e}}} \overline{d}_i^{\mathrm{v}} \overline{r}_{ij}^{\mathrm{v}} x_{ij}^{\mathrm{v}}(t) = \sum_{i\in\mathcal{A}_{\mathrm{e}}} f_{ij}^{\mathrm{v}} x_{ij}^{\mathrm{v}}(t) \tag{68}$$

$$= \sum_{i\in\mathcal{A}_{\mathrm{e}}\cup\mathcal{A}_{\mathrm{e}}} f_i^{\mathrm{v}} \overline{r}_{ij}^{\mathrm{v}} x_{ij}^{\mathrm{v}}(t) - \sum_{i\in\mathcal{A}_{\mathrm{i}}} f_j^{\mathrm{v}} \overline{r}_{jk}^{\mathrm{v}} x_{jk}^{\mathrm{v}}(t) \tag{69}$$

$$= \sum_{i\in\mathcal{A}_{\mathrm{e}}\cup\mathcal{A}_{\mathrm{e}}} f_i^{\mathrm{v}} \overline{r}_{ij}^{\mathrm{v}} x_{ij}^{\mathrm{v}}(t) - \sum_{j\in\Gamma_i^+} [f_i^{\mathrm{v}} \overline{r}_{ij}^{\mathrm{v}}] \sum_k \overline{r}_{jk}^{\mathrm{v}} x_{jk}^{\mathrm{v}}(t) \tag{70}$$

$$= \sum_{i\in\mathcal{A}_{\mathrm{i}}\cup\mathcal{A}_{\mathrm{e}}} f_i^{\mathrm{v}} \overline{r}_{ij}^{\mathrm{v}} (w_{ij}^{\mathrm{v}}(t)) \tag{71}$$

Combining Eqs. (66) and (71) yields

$$\begin{aligned}&\mathbb{E}[\mathbf{x}^{\mathrm{v}}(t)^{\mathrm{T}} \boldsymbol{\delta}(t) | \mathbf{x}^{\mathrm{v}}(t)] \\ &= \sum_{i\in\mathcal{A}_{\mathrm{i}}\cup\mathcal{A}_{\mathrm{e}}} (f_i^{\mathrm{v}} \overline{r}_{ij}^{\mathrm{v}} - \mathbb{E}[\min\{Q_{ij}^{\mathrm{v}} s_{ij}(t), x_{ij}^{\mathrm{v}}(t)\} | \mathbf{x}^{\mathrm{v}}(t)]) w_{ij}^{\mathrm{v}}(t)\end{aligned} \tag{72}$$

$$\begin{aligned}&= \sum_{i\in\mathcal{A}_{\mathrm{i}}\cup\mathcal{A}_{\mathrm{e}}} (f_i^{\mathrm{v}} \overline{r}_{ij}^{\mathrm{v}} - Q_{ij}^{\mathrm{v}} \overline{s}_{ij}) w_{ij}^{\mathrm{v}}(t) \\ &\quad + \sum_{i\in\mathcal{A}_{\mathrm{i}}\cup\mathcal{A}_{\mathrm{e}}} (Q_{ij}^{\mathrm{v}} \overline{s}_{ij} - \mathbb{E}[\min\{Q_{ij}^{\mathrm{v}} s_{ij}(t), x_{ij}^{\mathrm{v}}(t)\} | \mathbf{x}^{\mathrm{v}}(t)]) w_{ij}^{\mathrm{v}}(t)\end{aligned} \tag{73}$$

For the second term of Eq. (73), if $x_{ij}^{\mathrm{v}}(t) \geq Q_{ij}^{\mathrm{v}}$, then we have $\mathbb{E}[\min\{Q_{ij}^{\mathrm{v}} s_{ij}(t), x_{ij}^{\mathrm{v}}(t)\} | \mathbf{x}^{\mathrm{v}}(t)] = Q_{ij}^{\mathrm{v}} \overline{s}_{ij}$. Therefore, the second term of Eq. (73) equals zero. If $x_{ij}^{\mathrm{v}}(t) < Q_{ij}^{\mathrm{v}}$, then we have $\mathbb{E}[\min\{Q_{ij}^{\mathrm{v}} s_{ij}(t), x_{ij}^{\mathrm{v}}(t)\} | \mathbf{x}^{\mathrm{v}}(t)] = \mathbb{E}[x_{ij}^{\mathrm{v}}(t) | \mathbf{x}^{\mathrm{v}}(t)]$. Therefore, we obtain the following:

$$(Q_{ij}^{\mathrm{v}} \overline{s}_{ij} - \mathbb{E}[x_{ij}^{\mathrm{v}}(t) | \mathbf{x}^{\mathrm{v}}(t)]) w_{ij}^{\mathrm{v}}(t) \leq Q_{ij}^{\mathrm{v}} x_{ij}^{\mathrm{v}}(t) \leq (Q_{ij}^{\mathrm{v}})^2 \tag{74}$$

Hence, the second term of Eq. (73) equals zero or bounded by $\sum_{i\in\mathcal{A}_{\mathrm{i}}\cup\mathcal{A}_{\mathrm{e}}} (Q_{ij}^{\mathrm{v}})^2$.

The modified MP signal control $s_{ij}^*(t)$ is chosen from the feasible signal control set $\mathcal{S}$ satisfying pedestrian access, and $s_{ij}^*(t)$ seeks to maximize the objective of Eq. (61*a*). According to Lemma 2, we have

$$\begin{aligned}&\mathbb{E}\left[\sum_{i\in\mathcal{A}_{\mathrm{i}}\cup\mathcal{A}_{\mathrm{e}}} [f_i^{\mathrm{v}} \overline{r}_{ij}^{\mathrm{v}} - s_{ij}^*(t) Q_{ij}^{\mathrm{v}}] w_{ij}^{\mathrm{v}}(t) | w_{ij}^{\mathrm{v}}(t)\right] \\ &\leq \mathbb{E}\left[\sum_{i\in\mathcal{A}_{\mathrm{i}}\cup\mathcal{A}_{\mathrm{e}}} [f_i^{\mathrm{v}} \overline{r}_{ij}^{\mathrm{v}} - \overline{s}_{ij} Q_{ij}^{\mathrm{v}}] w_{ij}^{\mathrm{v}}(t) | w_{ij}^{\mathrm{v}}(t)\right]\end{aligned} \tag{75}$$

Therefore, for some feasible signal controls $s_{ij}(t)$ satisfying the stable region and integrated pedestrian phases, we obtain $\overline{s}_{ij}$ based on Eq. (10). We have

$$\sum_{i\in\mathcal{A}_{\mathrm{i}}\cup\mathcal{A}_{\mathrm{e}}} [f_i^{\mathrm{v}} \overline{r}_{ij}^{\mathrm{v}} - \overline{s}_{ij} Q_{ij}^{\mathrm{v}}] w_{ij}^{\mathrm{v}}(t) \leq -\epsilon \sum_{ij} \max\{w_{ij}^{\mathrm{v}}, 0\} \leq -\epsilon |w_{ij}^{\mathrm{v}}| \tag{76}$$

We know that the pressure $\mathbf{w}(t)$ is a linear function of the queue length of vehicles. So, we can find $\beta > 0$ to satisfy $\sum_{(i,j)\in\mathcal{M}^2} w_{ij}^{\mathrm{v}} \geq \beta |\mathbf{x}^{\mathrm{v}}|$. Then, we have

$$-\epsilon |w_{ij}^{\mathrm{v}}| \leq -\epsilon\beta |\mathbf{x}^{\mathrm{v}}| \leq \sum_{i\in\mathcal{A}_{\mathrm{i}}\cup\mathcal{A}_{\mathrm{e}}} (Q_{ij}^{\mathrm{v}})^2 - \epsilon\beta |\mathbf{x}^{\mathrm{v}}| \tag{77}$$

where $\delta_{ij}(t)$ is upper-bounded by $\max\{Q_{ij}^{\mathrm{v}}, \sum_{h\in\mathcal{A}_i^-} Q_{ij}^{\mathrm{v}}\}$, which is the same as Eq. (50). Based on Eq. (77), and Eqs. (50)–(56), we obtain

$$\begin{aligned}|\mathbf{x}^{\mathrm{v}}(t+1)|^2 - |\mathbf{x}^{\mathrm{v}}(t)|^2 &= 2\mathbf{x}^{\mathrm{v}}(t)^{\mathrm{T}} \boldsymbol{\delta} + |\boldsymbol{\delta}|^2 \\ &\leq 2\left(\sum_{i\in\mathcal{A}_{\mathrm{i}}\cup\mathcal{A}_{\mathrm{e}}} (Q_{ij}^{\mathrm{v}})^2 - \epsilon\beta |\mathbf{x}^{\mathrm{v}}(t)|\right) + \mathrm{M}\psi^2\end{aligned} \tag{78}$$

$$= \kappa - \eta |\mathbf{x}^{\mathrm{v}}(t)| \tag{79}$$

where $\kappa = 2\sum_{i\in\mathcal{A}_{\mathrm{i}}\cup\mathcal{A}_{\mathrm{e}}} (Q_{ij}^{\mathrm{v}})^2 + \mathrm{M}\psi^2$ and $\epsilon\beta = \psi$.

Proposition 4: Ped-MP is stabilizing when $\overline{\mathbf{d}}^{\mathrm{v}} \in \mathcal{D}^0$.

Proof: The proof is analogous to Proposition 3. Inequality Eq. (66) holds from Lemma 3. Taking expectations, summing over $t = 1, \ldots, T$, and transferring the position of terms gives the following inequality:

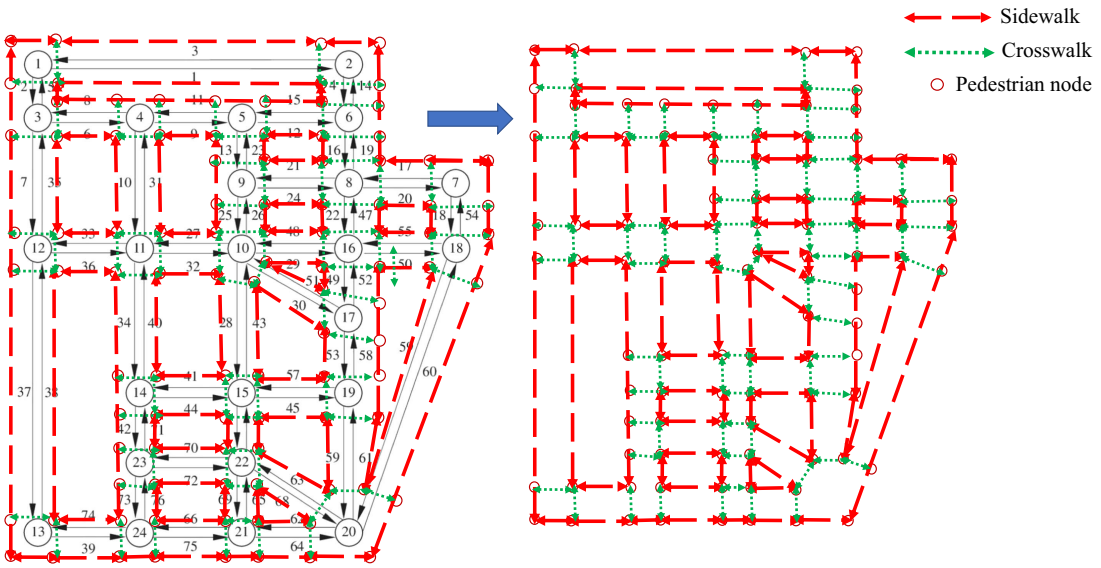

Fig. 4. Sioux Falls network with pedestrian access.

$$\eta\frac{1}{T}\sum_{t=1}^{T}\mathbb{E}[|\mathbf{x}^{v}(t)|] \le \kappa - \frac{1}{T}\mathbb{E}[\nu(T+1)] + \frac{1}{T}\mathbb{E}[\nu(1)]$$
$$\le \kappa + \frac{1}{T}\mathbb{E}[\nu(1)] \tag{80}$$

which satisfies Definition 1 for stability.

Multiple-Scenario Simulation and Numerical Results

To test the performance of the proposed Ped-MP, we set up simulations on the Sioux Falls network considering pedestrian access. Fig. 4 illustrates the pedestrian network based on the Sioux Falls network. There are 24 intersections and 72 links for vehicles, and 93 crosswalks for pedestrians in the Sioux Falls network. Hourly demand for the Sioux Falls network file is 15,025 vehicles/h. We randomly generate pedestrians at each pedestrian node, and their destination is another pedestrian node. The simulation is built in Java with IBM CPLEX optimization solver. We set the simulation duration at 4 h to ensure it is long enough to evaluate network stability. The main purpose of the simulation is to demonstrate stability performance when including pedestrian access.

Stable and Unstable Networks

Here, we compare the stability performance based on stable network definition, Definition 1. We test different demand under the same tolerance time. Fig. 5 shows the results for stable network and unstable network. When demand is within the stable region, the average queue length will remain bounded, while when demand is outside of stable region, the average queue length will increase with simulation running.

Stability Comparison

First, we demonstrate that the proposed Ped-MP can still achieve maximum throughput when considering pedestrian access. Fig. 6 shows the average queue length for a current fixed-time signal control with pedestrian access compared with Ped-MP with 120-s tolerance time. When we load 5,000 vehicles/h into the network, the average queue length for fixed-time controller increases to infinity,

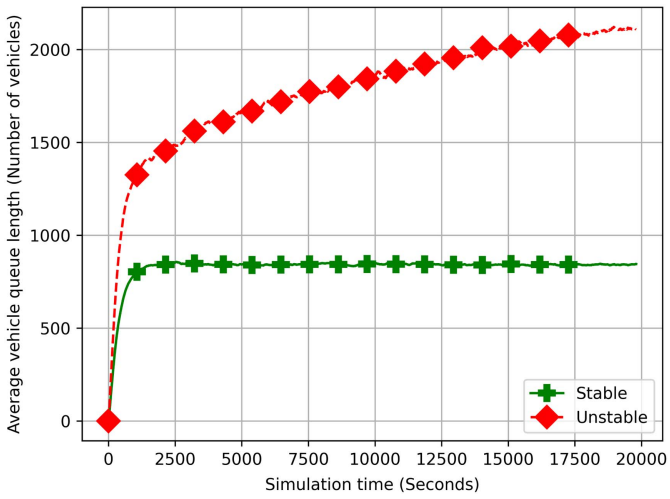

Fig. 5. Stable and unstable network.

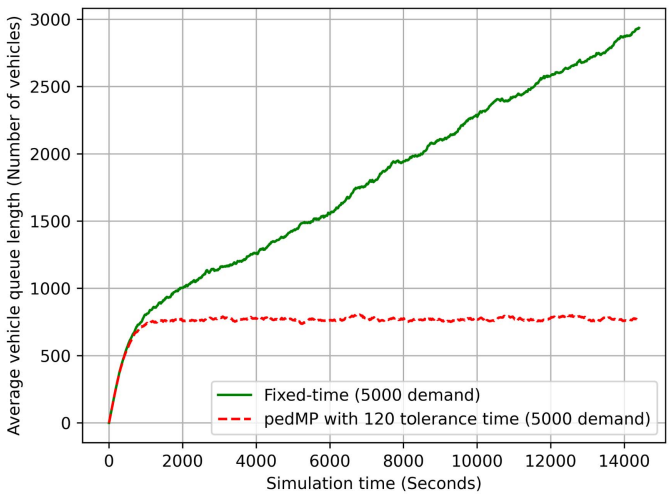

Fig. 6. Comparison between Ped-MP and fixed time controller.

J. Transp. Eng., Part A: Systems, 2024, 150(7): 04024028

but Ped-MP can still stabilize the network while including pedestrian access, which is consistent with Proposition 4.

After considering pedestrian access, we have to occupy some signal timing that could be used for vehicles. It would be interesting to check the throughput loss after considering pedestrian access with difference tolerance time. Therefore, we simulate Ped-MP with 30-s, 60-s, 90-s, and 120-s tolerance under different vehicle demand to find the maximum stable region for each Ped-MP controller and throughput loss. Figs. 7(a–d) show that higher tolerance times for pedestrians increase the stable region for vehicles. In Fig. 7(a), the stable region for Ped-MP with a 30-s tolerance setting is approximately 3,000 vehicles/h. For demands exceeding this threshold, we observe an escalation in the average queue length as the simulation progresses. Similarly, for Fig. 7(b), the stable threshold is about 4,000 vehicles/h given a 60-s tolerance setting. When demands surpass this, a noticeable rise occurs in the average queue length with ongoing simulation time. In Fig. 7(c), with a 90-s tolerance setting, the stable region is around 5,000 vehicles/h. Beyond this demand, the average queue length exhibits growth. Last, Fig. 7(d) indicates that the stable region is approximately 5,750 vehicles per hour for Ped-MP with a 120-s tolerance. Once again, for demands beyond this limit, the average queue length demonstrates an upward trend as the simulation continues. Therefore, we can see the throughput loss lower tolerance times.

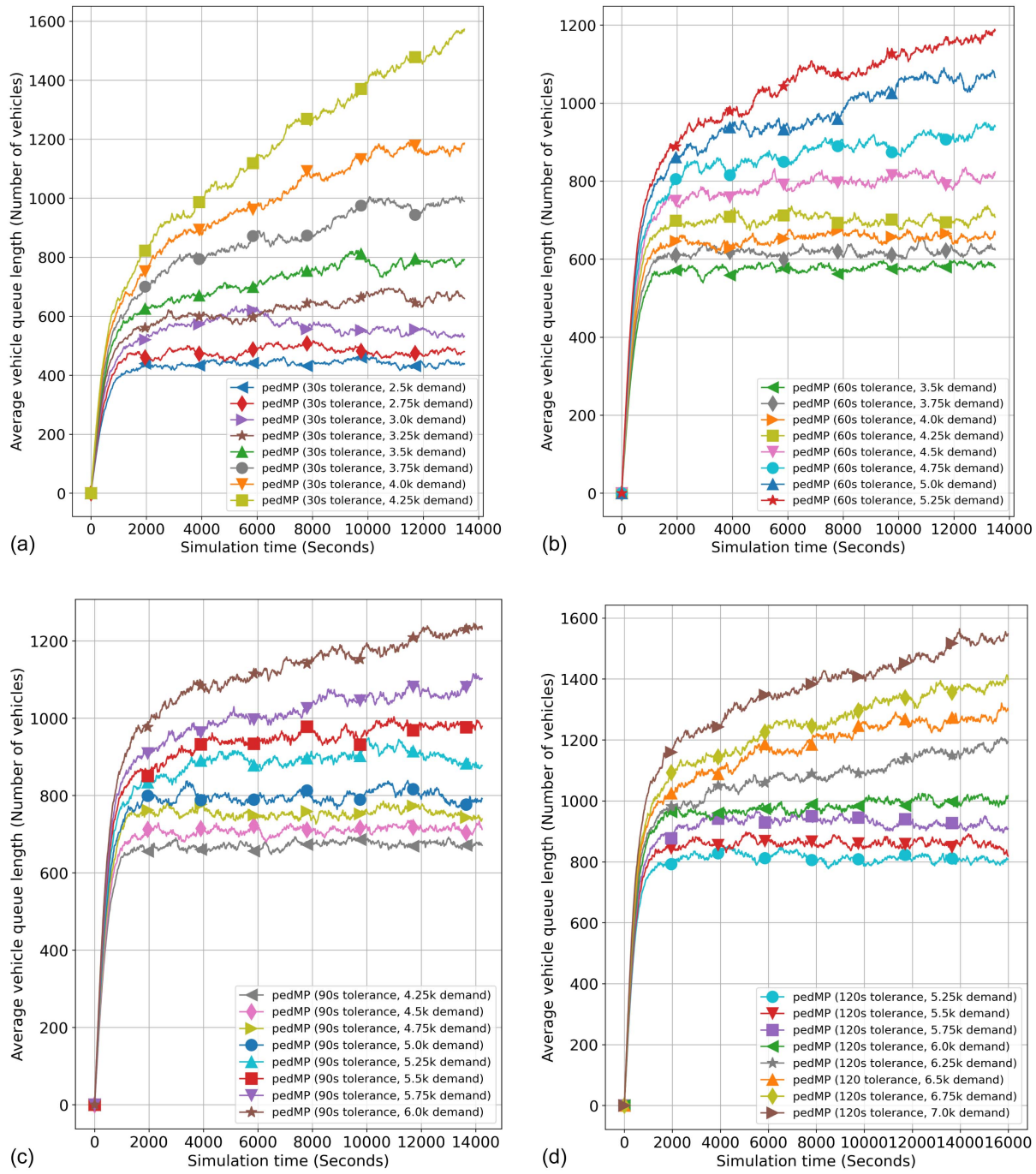

Fig. 7. Throughput loss analysis: (a) Ped-MP with 30 s tolerance time under different demand; (b) Ped-MP with 60 s tolerance time under different demand; (c) Ped-MP with 90 s tolerance time under different demand; and (d) Ped-MP with 1,200 s tolerance time under different demand.

J. Transp. Eng., Part A: Systems, 2024, 150(7): 04024028

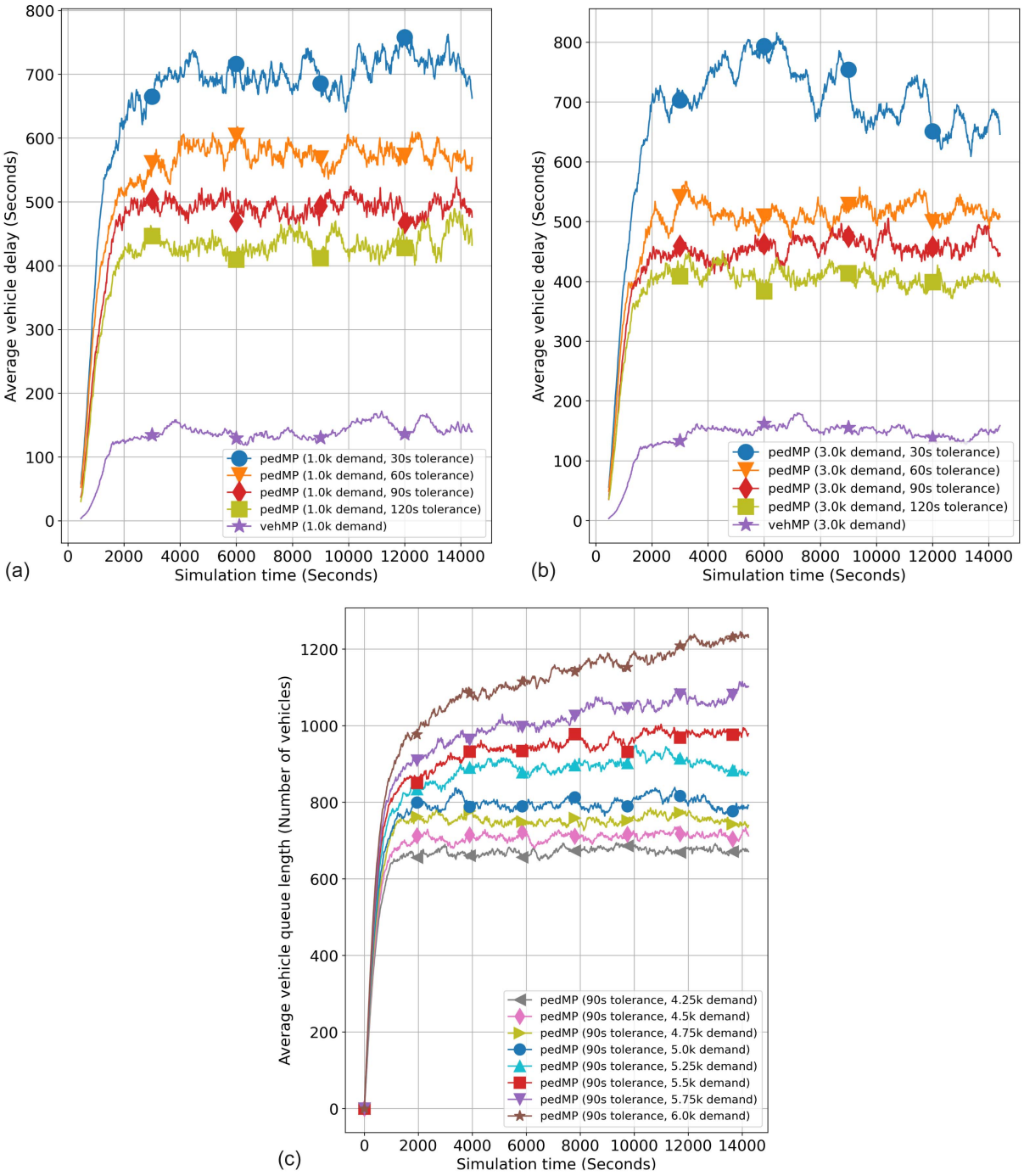

Fig. 8. Average vehicle delay: (a) 1,000 vehicles hourly demand; (b) 3,000 vehicles hourly demand; and (c) 5,000 vehicles hourly demand.

Vehicle Delay

Vehicle delay is one of the most important indicators to evaluate the signal control performance, which has been used in recent MP control research (Li and Jabari 2019; Wang et al. 2022; Xu et al. 2022a, b, c). Here, we provide average vehicle delay dynamics under different pedestrian tolerance times (30, 60, 90, and 120 s) and different vehicle demand settings (1,000, 3,000, and 5,000 vehicles/h) to determine how these factors influence vehicle delay. Fig. 8 shows that under different demand, average vehicle delay is lowest with the original MP control proposed by Varaiya (2013), and when tolerance times increase the vehicle delay decreases, because vehicles have more time to use intersections. Specifically, when demand is larger, for example, 5,000 vehicles/h as in Fig. 8(c), vehicle delay for Ped-MP with 30-s tolerance time will increase arbitrary large value, but for other tolerance times, vehicle delay fluctuates around a constant.

In Fig. 9, we elucidate the relationship between vehicle delay and demand across various tolerance time settings. This figure illustrates a pronounced impact of tolerance time on vehicle delay: As the tolerance time decreases, the vehicle delay increases. Furthermore, the sensitivity of vehicle delay to changes in demand also escalates with shorter tolerance times. For instance, an increase in demand does not significantly alter the vehicle delay when the tolerance times are set at 90 s, 120 s, or under the original MP control. In stark contrast, for tolerance times of 30 and 60 s, we observe a dramatic surge in vehicle delay as demand rises from 1,000 to 5,000 vehicles/h.

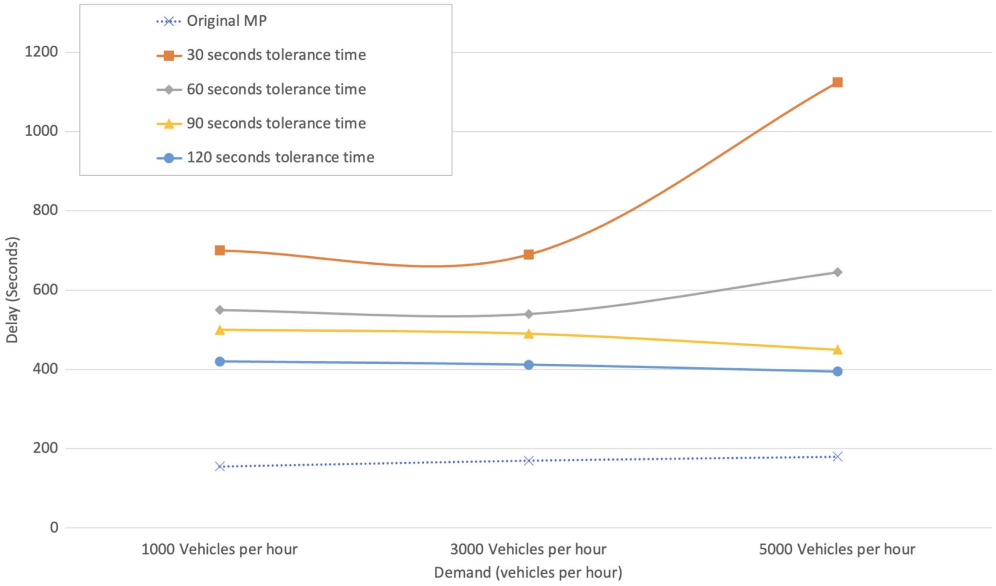

Fig. 9. Delay-demand-tolerance time.

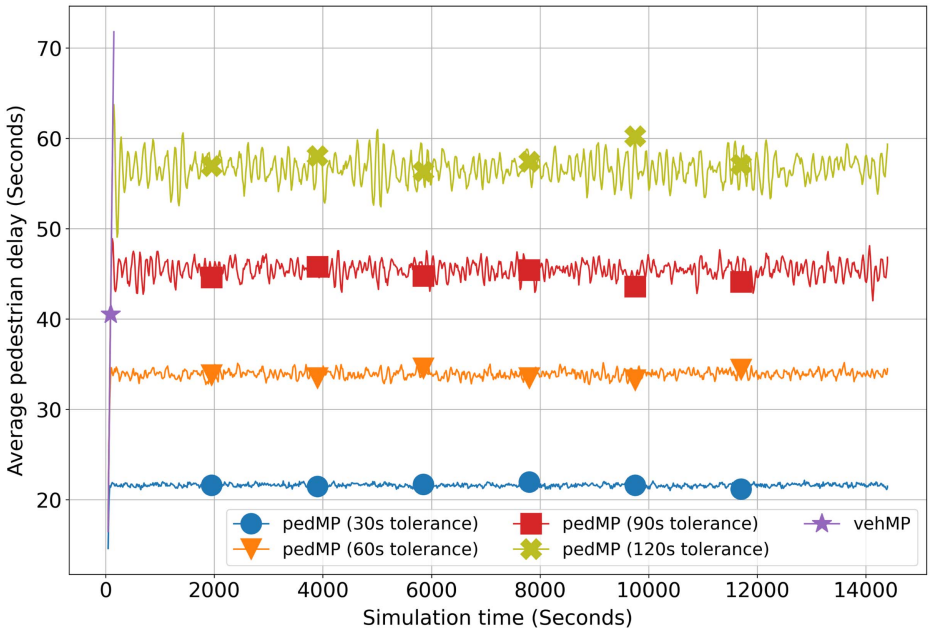

Fig. 10. Impacts on pedestrian delay.

Impacts on Pedestrians

One of the major goals of this work is to provide a pedestrian-friendly MP control, which means we can bound pedestrian waiting times around intersections. Therefore, we want to check how Ped-MP impacts pedestrians. We provide average pedestrian delays for exploration. We simulate with 3,000 vehicles/h demand, which is in the stable region for all Ped-MP controllers under different tolerance times. Pedestrians are generated around average intersections every time they step into the network, and they have a random path, which means some of them will walk through the crosswalks and some will walk through sidewalks. Under these simulation scenarios, we add many pedestrians around each signal intersection to have a significantly high pedestrian demand. In this way, we provide a persuasive way to check how Ped-MP performs. Fig. 10 provides detailed results. Unsurprisingly, the original MP control, which was proposed by Varaiya (2013), is not "friendly" to pedestrians. The delay of pedestrians increases quickly to a significantly higher value compared with all Ped-MP under different tolerance times. Also, the higher the tolerance time, the higher the pedestrian delay. For the 30-s tolerance time, the average delay for pedestrians fluctuates around 20 s. For the 60-s tolerance time, the average pedestrian delay fluctuates around 35 s, and for 90- and 120-s tolerance time, the average delay is around 45 s and 55 s, respectively. These results demonstrate that it is important to consider pedestrian access if we want to provide a more practical MP controller in the future, because there are large pedestrian cross demands in cities, especially in central business districts, and our proposed Ped-MP achieves good results on pedestrian delay.

Conclusions

Most previous studies about MP control policy only consider the vehicle network. There are only two previous studies that tried to include multiple modes in MP control (Chen et al. 2020; Xu et al. 2022b). To boost the scope of application of MP control, we proposed a pedestrian-friendly max-pressure signal controller, Ped-MP, for the first time. Moreover, we built a pedestrian network based on the Sioux Falls network, which makes our simulation more realistic than previous studies. We also analytically proved that our novel Ped-MP can still achieve maximum stability.

The numerical analysis conducted on the Sioux Falls network indicates that a reduction in the tolerance time correlates with decreased delays for pedestrians. It is not surprising that the performance of vehicles is best under original MP control proposed by Varaiya (2013), but these results demonstrate that we need to sacrifice vehicle performance for pedestrian access. The lower the tolerance time, the more throughput loss in network. However, we find pedestrians have much less delay when we implement Ped-MP, even when we have a large number of pedestrians in the network, which means our proposed Ped-MP can provide more walkable spaces in cities and bound pedestrian waiting time in the cities. Overall, the proposed Ped-MP can serve as much vehicle demand whenever possible while including pedestrian access, which is more friendly to practical traffic operations.

In the future, there are still many extensions to consider. For example, including the information, such as number of pedestrian waiting for crossing, by advanced infrastructure sensors, will help us provide more accurate information for MP signal timing consider pedestrian access. Integrating adaptive cruise control into MP control would be an interesting topic to explore (Li et al. 2023b). In addition, the results will benefit more from the design of pedestrian walking space, such as the design of crosswalks for pedestrian access, especially for the disabled.

Data Availability Statement

Some or all data, models, or code that support the findings of this study are available from the corresponding author upon reasonable request.

Acknowledgments

The authors gratefully acknowledge the support of the National Science Foundation, Award No. 1935514 and the support of Hsiao Shaw-Lundquist Fellowship of the University of the Minnesota China Center. The authors also gratefully acknowledge the amazing book written by Boyles et al. (2023). The core concept, knowledge, and coding design were leveraged from Chapter 9, Dynamic Network Loading.

Author contributions: The authors confirm contribution to the paper as follows: T. Xu and M. Levin: conception. T. Xu and M. Levin: methodology. B. Yashveer and T. Xu: software, experiment design, and simulation. B. Yashveer: visualization. T. Xu and B. Yashveer: analysis and interpretation of results. T. Xu, B. Yashveer, and M. Levin: draft manuscript preparation. T. Xu, B. Yashveer, and M. Levin: validation. T. Xu, B. Yashveer, and M. Levin: writing review and editing. M. Levin: supervision. M. Levin: funding acquisition. All authors reviewed the results and approved the final version of the manuscript.

Notation

The following symbols are used in this paper:

$\mathcal{A}$ = set of links (including vehicle links $\mathcal{A}^{\mathrm{v}}$ and pedestrian links $\mathcal{A}^{\mathrm{p}}$);
$d_i^{\mathrm{p}}(t)$ = pedestrian demand at entry link i;
$d_i^{\mathrm{v}}(t)$ = vehicle demand at entry link i;
f_i^{v} = average vehicle traffic volume of link i;
$\mathcal{M}$ = set of movements (vehicle movements $\mathcal{M}^{\mathrm{v}}$, pedestrian movement $\mathcal{M}^{\mathrm{p}}$);
$\mathcal{N}$ = set of nodes (including vehicle nodes $\mathcal{N}^{\mathrm{v}}$ and pedestrian nodes $\mathcal{N}^{\mathrm{p}}$);
Q_c = capacity of conflict region;
Q_{ij}^{v} = capacity of turning movement for private vehicles from link i to link j;
$r_{ij}^{\mathrm{v}}(t)$ = proportion of vehicles entering i that will next move to j;
$r_{ij}^{\mathrm{p}}(t)$ = proportion of pedestrians entering i that will next move to j;
$s_{ij}(t)$ = actuation of turning movement from link i to link j at time step t;
$s_{mb}(t)$ = actuation of crosswalk from pedestrian link m to b at time step t;
$w_{ij}^{\mathrm{v}}(t)$ = weight of vehicle turning movement from link i to link j at time step t;
$x_{ij}^{\mathrm{p}}(t)$ = number of pedestrians of the movement from link i to link j at time step t;
$x_{ij}^{\mathrm{v}}(t)$ = number of vehicles of the movement from link i to link j at time step t;
$y_{ij}^{\mathrm{p}}(t)$ = signal control number of pedestrians from link i to link j at time step t;
$y_{ij}^{\mathrm{v}}(t)$ = signal control vehicle flow from link i to link j at time step t;
α_{ij}^{b} = 0–1 binary dummy variable ($\alpha_{ij}^{b} = 1$ when vehicles have conflict with crosswalk b);
$\lambda_{\mathbf{s}}$ = proportion of time spent in each phase $\mathbf{s}$ ($\sum_{\mathbf{s}} \lambda_{\mathbf{s}} = 1$);
Γ_j^{+} = set of outgoing links; and
Γ_j^{-} = set of incoming links.

References

Akyol, G., I. G. Erdagi, M. A. Silgu, and H. B. Celikoglu. 2020. "Adaptive signal control to enhance effective green times for pedestrians: A case study." *Transp. Res. Procedia* 47 (Jan): 704–711. https://doi.org/10.1016/j.trpro.2020.03.150.

Barman, S., and M. W. Levin. 2022. "Performance evaluation of modified cyclic max-pressure controlled intersections in realistic corridors." *Transp. Res. Rec.* 2676 (6): 110–128. https://doi.org/10.1177/03611981211072807.

Boyles, S. D., N. E. Lownes, and A. Unnikrishnan. 2023. "Transportation network analysis." Accessed August 21, 2023. https://sboyles.github.io/teaching/ce392c/book.pdf.

Cafiso, S., A. G. Garcia, R. Cavarra, and M. Rojas. 2011. "Crosswalk safety evaluation using a pedestrian risk index as traffic conflict measure." In *Proc., 3rd Int. Conf. on Road Safety and Simulation*, 1–15. Alexandria, VA: Engineering, Environmental Science.

Chang, W., D. Roy, S. Zhao, A. Annaswamy, and S. Chakraborty. 2020. "Cps-oriented modeling and control of traffic signals using adaptive back pressure." In *Proc., 2020 Design, Automation & Test in Europe Conf. & Exhibition (DATE)*, 1686–1691. New York: IEEE.

Chen, R., J. Hu, M. W. Levin, and D. Rey. 2020. "Stability-based analysis of autonomous intersection management with pedestrians." *Transp. Res. Part C Emerging Technol.* 114 (May): 463–483. https://doi.org/10.1016/j.trc.2020.01.016.

Dixit, V., D. J. Nair, S. Chand, and M. W. Levin. 2020. "A simple crowdsourced delay-based traffic signal control." *PLoS One* 15 (4): e0230598. https://doi.org/10.1371/journal.pone.0230598.

DOT. 2019. *Traffic safety facts 2019*. Washington, DC: DOT.

Gregoire, J., E. Frazzoli, A. de La Fortelle, and T. Wongpiromsarn. 2014a. "Back-pressure traffic signal control with unknown routing rates." *IFAC Proc.* 47 (3): 11332–11337. https://doi.org/10.3182/20140824-6-ZA-1003.01585.

Gregoire, J., X. Qian, E. Frazzoli, A. De La Fortelle, and T. Wongpiromsarn. 2014b. "Capacity-aware backpressure traffic signal control." *IEEE Trans. Control Network Syst.* 2 (2): 164–173. https://doi.org/10.1109/TCNS.2014.2378871.

He, Q., K. L. Head, and J. Ding. 2012. "Pamscod: Platoon-based arterial multi-modal signal control with online data." *Transp. Res. Part C Emerging Technol.* 20 (1): 164–184. https://doi.org/10.1016/j.trc.2011.05.007.

He, Q., K. L. Head, and J. Ding. 2014. "Multi-modal traffic signal control with priority, signal actuation and coordination." *Transp. Res. Part C Emerging Technol.* 46 (Sep): 65–82. https://doi.org/10.1016/j.trc.2014.05.001.

Heinrichs, D., and J. Jarass. 2020. "Designing healthy mobility in cities: How urban planning can promote walking and cycling." *Bundesgesundheitsbl. Gesundheitsforsch. Gesundheitsschutz* 63 (Aug): 945–952. https://doi.org/10.1007/s00103-020-03180-1.

Hooper, P., B. Boruff, B. Beesley, H. Badland, and B. Giles-Corti. 2018. "Testing spatial measures of public open space planning standards with walking and physical activity health outcomes: Findings from the Australian national liveability study." *Landscape Urban Plann.* 171 (Mar): 57–67. https://doi.org/10.1016/j.landurbplan.2017.12.001.

Ke, Z., Z. Li, Z. Cao, and P. Liu. 2020. "Enhancing transferability of deep reinforcement learning-based variable speed limit control using transfer learning." *IEEE Trans. Intell. Transp. Syst.* 22 (7): 4684–4695. https://doi.org/10.1109/TITS.2020.2990598.

Khosravi, S., B. Beak, K. L. Head, and F. Saleem. 2018. "Assistive system to improve pedestrians' safety and mobility in a connected vehicle technology environment." *Transp. Res. Rec.* 2672 (19): 145–156. https://doi.org/10.1177/0361198118783598.

Le, T., P. Kovács, N. Walton, H. L. Vu, L. L. Andrew, and S. S. Hoogendoorn. 2015. "Decentralized signal control for urban road networks." *Transp. Res. Part C Emerging Technol.* 58 (Sep): 431–450. https://doi.org/10.1016/j.trc.2014.11.009.

Leden, L., P. Gårder, and C. Johansson. 2006. "Safe pedestrian crossings for children and elderly." *Accid. Anal. Prev.* 38 (2): 289–294. https://doi.org/10.1016/j.aap.2005.09.012.

Levin, M. W., J. Hu, and M. Odell. 2020. "Max-pressure signal control with cyclical phase structure." *Transp. Res. Part C Emerging Technol.* 120 (Nov): 102828. https://doi.org/10.1016/j.trc.2020.102828.

Levin, M. W., D. Rey, and A. Schwartz. 2019. "Max-pressure control of dynamic lane reversal and autonomous intersection management." *Transportmetrica B: Transport Dyn.* 7 (1): 1693–1718. https://doi.org/10.1016/j.trc.2020.102828.

Li, L., and S. E. Jabari. 2019. "Position weighted backpressure intersection control for urban networks." *Transp. Res. Part B Methodol.* 128 (Oct): 435–461. https://doi.org/10.1016/j.trb.2019.08.005.

Li, T., J. Klavins, T. Xu, N. M. Zafri, and R. Stern. 2023a. "Understanding driver-pedestrian interactions to predict driver yielding: Naturalistic open-source dataset collected in Minnesota." Preprint, submitted December 22, 2023. http://arxiv.org/abs/2312.15113.

Li, T., B. Rosenblad, S. Wang, M. Shang, and R. Stern. 2023b. "Exploring energy impacts of cyberattacks on adaptive cruise control vehicles." In *Proc., 2023 IEEE Intelligent Vehicles Symp. (IV)*, 1–6. New York: IEEE.

Liang, M., Y. Chao, Y. Tu, and T. Xu. 2023. "Vehicle pollutant dispersion in the urban atmospheric environment: A review of mechanism, modeling, and application." *Atmosphere* 14 (2): 279. https://doi.org/10.3390/atmos14020279.

Liu, H., and V. V. Gayah. 2022. "A novel max pressure algorithm based on traffic delay." Preprint, submitted February 7, 2022. http://arxiv.org/abs/2202.03290.

Ma, K., and H. Wang. 2021. "How connected and automated vehicle–exclusive lanes affect on-ramp junctions." *J. Transp. Eng. Part A Syst.* 147 (2): 04020157. https://doi.org/10.1061/JTEPBS.0000484.

Ma, K., H. Wang, and T. Ruan. 2021. "Analysis of road capacity and pollutant emissions: Impacts of connected and automated vehicle platoons on traffic flow." *Physica A* 583 (Dec): 126301. https://doi.org/10.1016/j.physa.2021.126301.

Ma, K., H. Wang, Z. Zuo, Y. Hou, X. Li, and R. Jiang. 2022. "String stability of automated vehicles based on experimental analysis of feedback delay and parasitic lag." *Transp. Res. Part C Emerging Technol.* 145 (Dec): 103927. https://doi.org/10.1016/j.trc.2022.103927.

Ma, W., D. Liao, Y. Liu, and H. K. Lo. 2015. "Optimization of pedestrian phase patterns and signal timings for isolated intersection." *Transp. Res. Part C Emerging Technol.* 58 (Sep): 502–514. https://doi.org/10.1016/j.trc.2014.08.023.

Maipradit, A., T. Kawakami, Y. Liu, J. Gao, and M. Ito. 2021. "An adaptive traffic signal control scheme based on back-pressure with global information." *J. Inf. Process.* 29 (Aug): 124–131. https://doi.org/10.2197/ipsjjip.29.124.

Manolis, D., T. Pappa, C. Diakaki, I. Papamichail, and M. Papageorgiou. 2018. "Centralised versus decentralised signal control of large-scale urban road networks in real time: A simulation study." *IET Int. Transp. Syst.* 12 (8): 891–900. https://doi.org/10.1049/iet-its.2018.0112.

Mercader, P., W. Uwayid, and J. Haddad. 2020. "Max-pressure traffic controller based on travel times: An experimental analysis." *Transp. Res. Part C Emerging Technol.* 110 (Jan): 275–290. https://doi.org/10.1016/j.trc.2019.10.002.

Park, Y., and M. Garcia. 2020. "Pedestrian safety perception and urban street settings." *Int. J. Sustainable Transp.* 14 (11): 860–871. https://doi.org/10.1080/15568318.2019.1641577.

Rey, D., and M. W. Levin. 2019. "Blue phase: Optimal network traffic control for legacy and autonomous vehicles." *Transp. Res. Part B Methodol.* 130 (Dec): 105–129. https://doi.org/10.1016/j.trb.2019.11.001.

Sun, X., and Y. Yin. 2018. "A simulation study on max pressure control of signalized intersections." *Transp. Res. Rec.* 2672 (18): 117–127. https://doi.org/10.1177/0361198118786840.

Tang, B.-S., K. K. Wong, K. S. Tang, and S. Wai Wong. 2021. "Walking accessibility to neighbourhood open space in a multi-level urban environment of Hong Kong." *Environ. Plann. B: Urban Anal. City Sci.* 48 (5): 1340–1356. https://doi.org/10.1177/2399808320932575.

Tassiulas, L., and A. Ephremides. 1990. "Stability properties of constrained queueing systems and scheduling policies for maximum throughput in multihop radio networks." In *Proc., 29th IEEE Conf. on Decision and Control*, 2130–2132. New York: IEEE.

Tu, Y., W. Wang, Y. Li, C. Xu, T. Xu, and X. Li. 2019. "Longitudinal safety impacts of cooperative adaptive cruise control vehicle's degradation." *J. Saf. Res.* 69 (Jun): 177–192. https://doi.org/10.1016/j.jsr.2019.03.002.

Varaiya, P. 2013. "Max pressure control of a network of signalized intersections." *Transp. Res. Part C Emerging Technol.* 36 (Nov): 177–195. https://doi.org/10.1016/j.trc.2013.08.014.

Vickrey, W. S. 1969. "Congestion theory and transport investment." *Am. Econ. Rev.* 59 (2): 251–260.

Wang, X., Y. Yin, Y. Feng, and H. X. Liu. 2022. "Learning the max pressure control for urban traffic networks considering the phase switching loss." *Transp. Res. Part C Emerging Technol.* 140 (Jul): 103670. https://doi.org/10.1016/j.trc.2022.103670.

Wei, H., C. Chen, G. Zheng, K. Wu, V. Gayah, K. Xu, and Z. Li. 2019. "Presslight: Learning max pressure control to coordinate traffic signals in arterial network." In *Proc., 25th ACM SIGKDD Int. Conf. on Knowledge Discovery & Data Mining*, 1290–1298. London: Special Interest Group on Knowledge Discovery in Data.

Wuthishuwong, C., and A. Traechtler. 2013. "Vehicle to infrastructure based safe trajectory planning for autonomous intersection management." In *Proc., 2013 13th Int. Conf. on ITS Telecommunications (ITST)*, 175–180. New York: IEEE.

Xu, K., J. Huang, L. Kong, J. Yu, and G. Chen. 2022a. "PV-TSC: Learning to control traffic signals for pedestrian and vehicle traffic in 6g era." *IEEE Trans. Intell. Transp. Syst.* 2022 (Mar): 14. https://doi.org/10.1109/TITS.2022.3156816.

Xu, T. 2023. "Boosting max-pressure signal control into practical implementation: Methodologies and simulation studies in city networks." Ph.D. thesis, Dept. of Civil, Environmental, and Geo-Engineering, Univ. of Minnesota.

Xu, T., S. Barman, M. W. Levin, R. Chen, and T. Li. 2022b. "Integrating public transit signal priority into max-pressure signal control: Methodology and simulation study on a downtown network." *Transp. Res. Part C Emerging Technol.* 138 (May): 103614. https://doi.org/10.1016/j.trc.2022.103614.

Xu, T., Y. Bika, and M. Levin. 2022c. *An approximate position-weighted back-pressure traffic signal control policy for traffic networks*. Amsterdam, Netherlands: Elsevier. https://doi.org/10.2139/ssrn.4186584.

Xu, T., M. Cieniawski, and M. W. Levin. 2023. "FMS-dispatch: A fast maximum stability dispatch policy for shared autonomous vehicles including exiting passengers under stochastic travel demand." *Transp. A: Transp. Sci.* 2023 (May): 1–39. https://doi.org/10.1080/23249935.2023.2214968.

Xu, T., M. W. Levin, and M. Cieniawski. 2021. "A zone-based dynamic queueing model and maximum-stability dispatch policy for shared autonomous vehicles." In *Proc., 2021 IEEE Int. Intelligent Transportation Systems Conf. (ITSC)*, 3827–3832. New York: IEEE.

Yang, M., Z. Li, Z. Ke, and M. Li. 2019. "A deep reinforcement learning-based ramp metering control framework for improving traffic operation at freeway weaving sections." In *Proc., Transp. Research Board 98th Annual Meeting*, 13–17. Washington, DC: National Academy of Sciences, Engineering, and Medicine.

Yu, H., P. Liu, Y. Fan, and G. Zhang. 2021. "Developing a decentralized signal control strategy considering link storage capacity." *Transp. Res. Part C Emerging Technol.* 124 (Mar): 102971. https://doi.org/10.1016/j.trc.2021.102971.

Zhang, H., Y. Nie, and Z. Qian. 2013. "Modelling network flow with and without link interactions: The cases of point queue, spatial queue and cell transmission model." *Transp. B: Transp. Dyn.* 1 (1): 33–51. https://doi.org/10.1080/21680566.2013.785921.

Zhang, Y., K. Gao, Y. Zhang, and R. Su. 2018. "Traffic light scheduling for pedestrian-vehicle mixed-flow networks." *IEEE Trans. Intell. Transp. Syst.* 20 (4): 1468–1483. https://doi.org/10.1109/TITS.2018.2852646.

Zhang, Y., Y. Zhang, and R. Su. 2019. "Pedestrian-safety-aware traffic light control strategy for urban traffic congestion alleviation." *IEEE Trans. Intell. Transp. Syst.* 22 (1): 178–193. https://doi.org/10.1109/TITS.2019.2955752.

Zheng, S., et al. 2023. "Coordinated variable speed limit control for consecutive bottlenecks on freeways using multiagent reinforcement learning." *J. Adv. Transp.* 2023 (Jun): 27. https://doi.org/10.1155/2023/4419907.